Neutron Star Crusts and Entrainment Effects

Kei Iida (Kochi University)

Contents

- *Introduction: Matter in the crust of a neutron star*
- *Pulsar glitches and magnetar quasiperiodic oscillations (QPOs)*
- *Trapped cold atoms as quantum simulators*
- *Working group on entrainment effects in A3 foresight project*
- *More on magnetar QPOs*

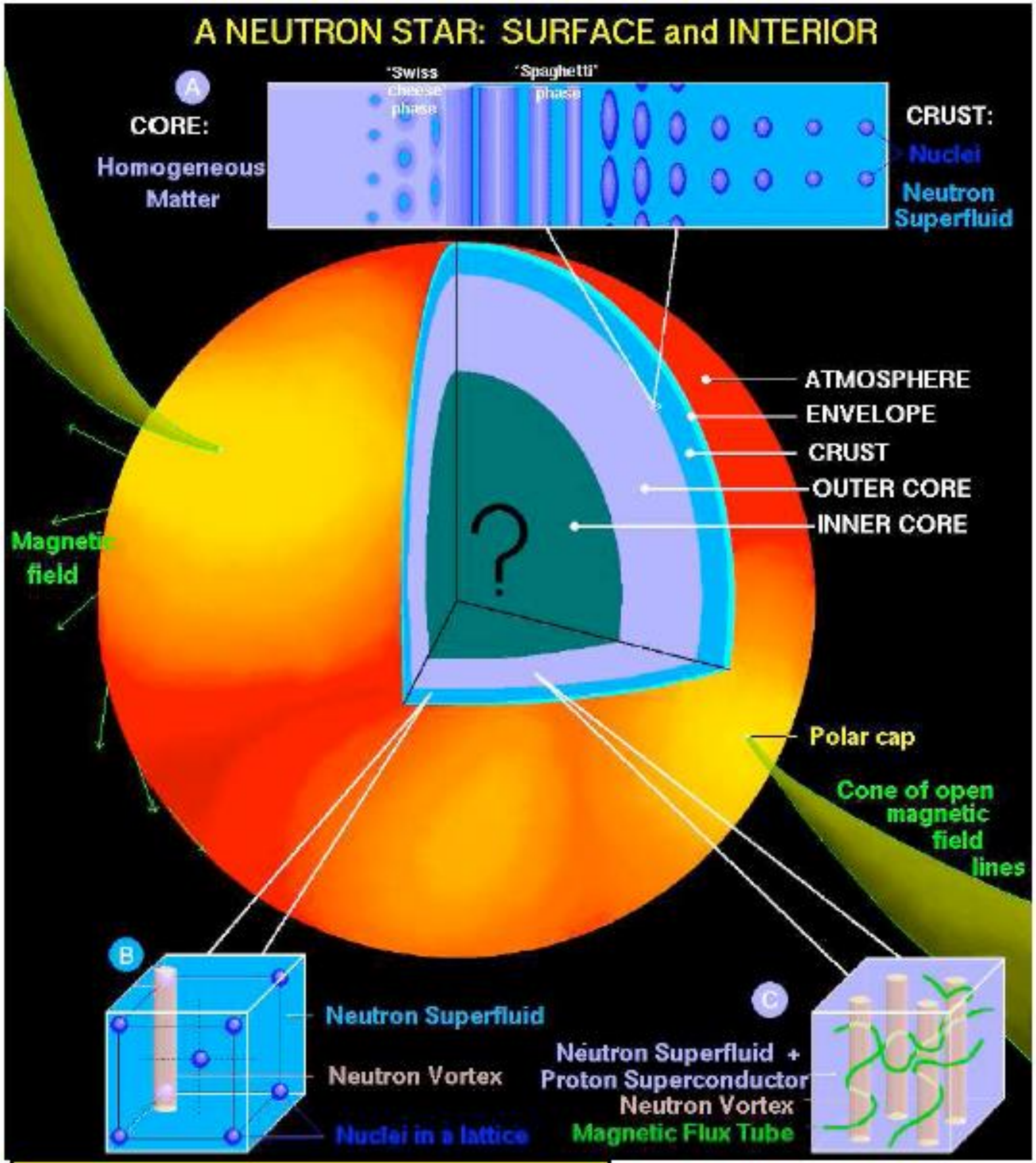

Lattimer and Prakash, astro-ph0405262

Figure by D. Page

Schematic phase diagram of dense matter

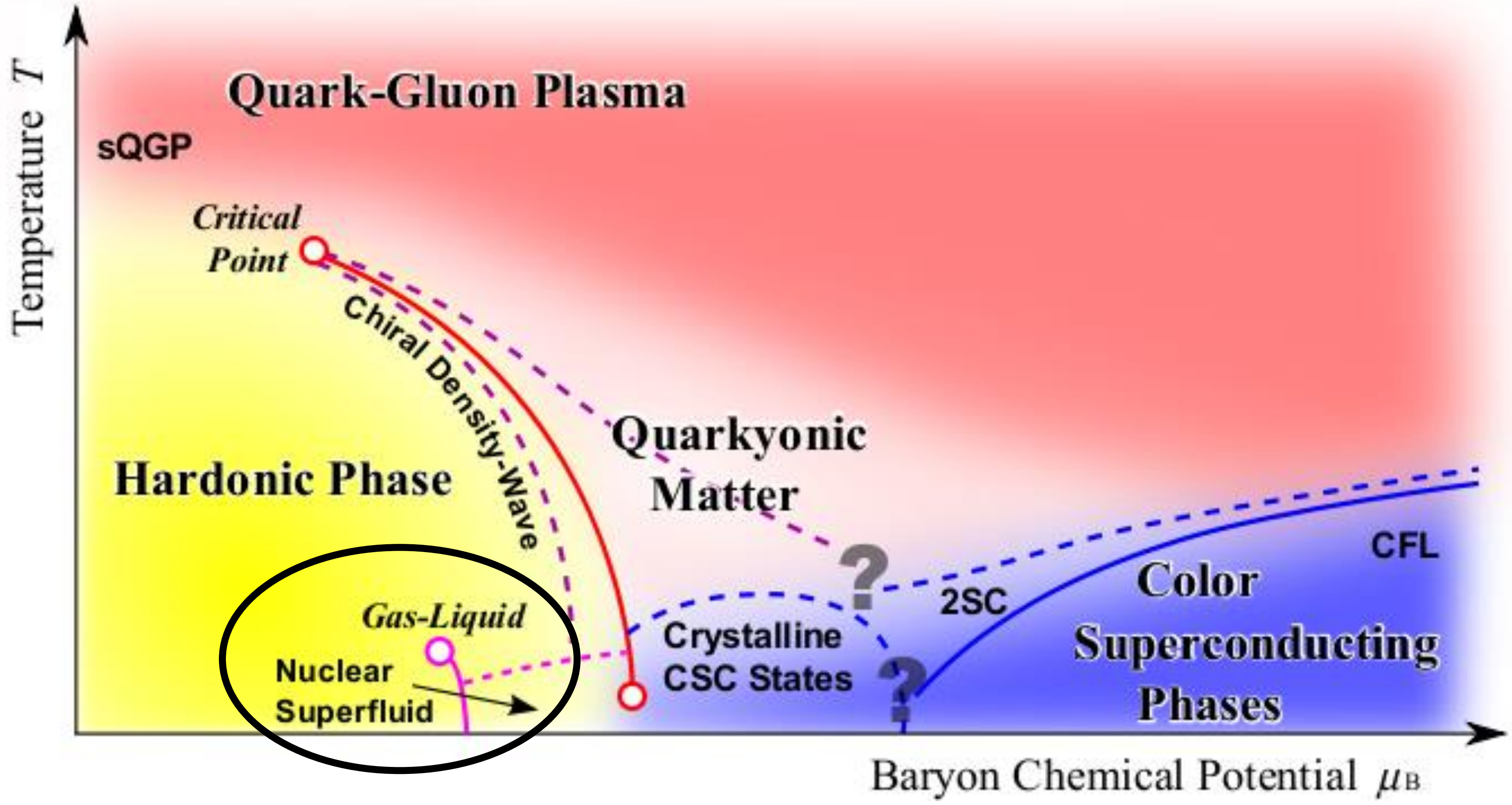

By Fukushima

Nuclear matter in neutron stars

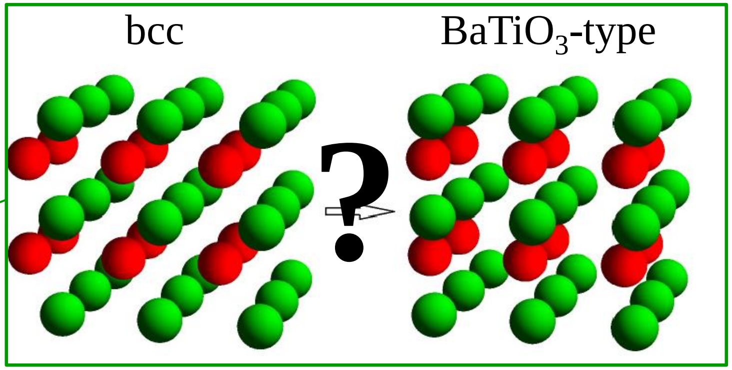

From Kobyakov and Pethick (2013, 2016).

Schematic cross-section of a neutron star

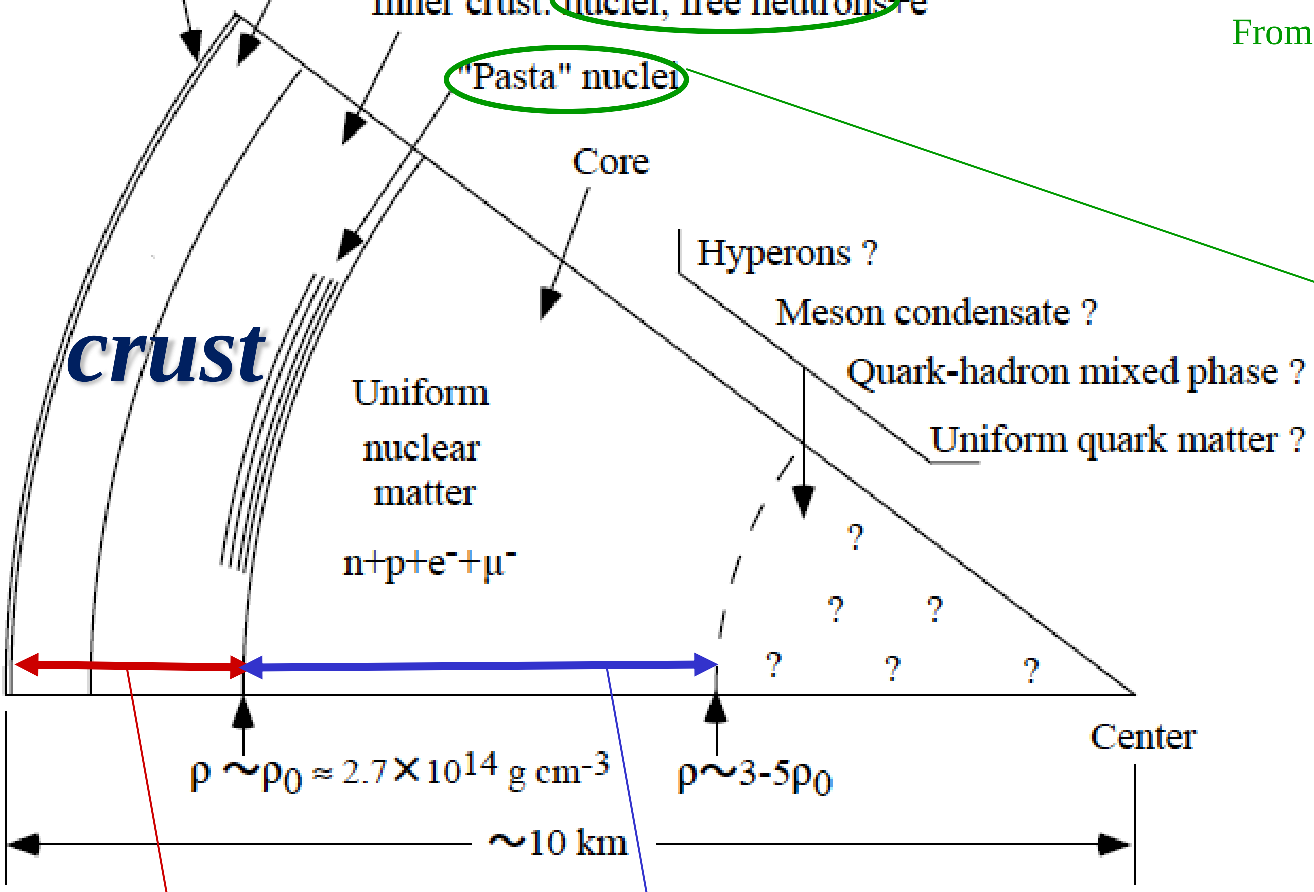

crust

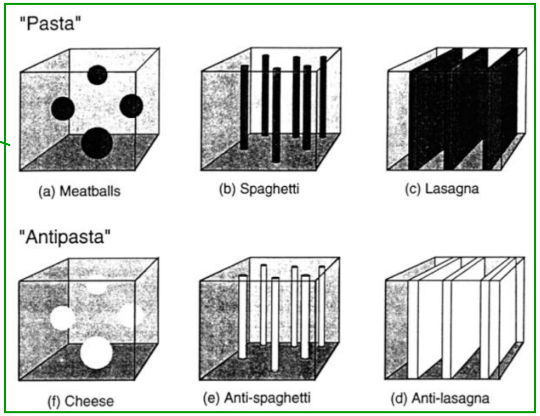

From Lamb (1991).

Liquid-gas mixture

Liquid

$T < \sim 10^9$ K（cold）

Systems composed of nuclear matter

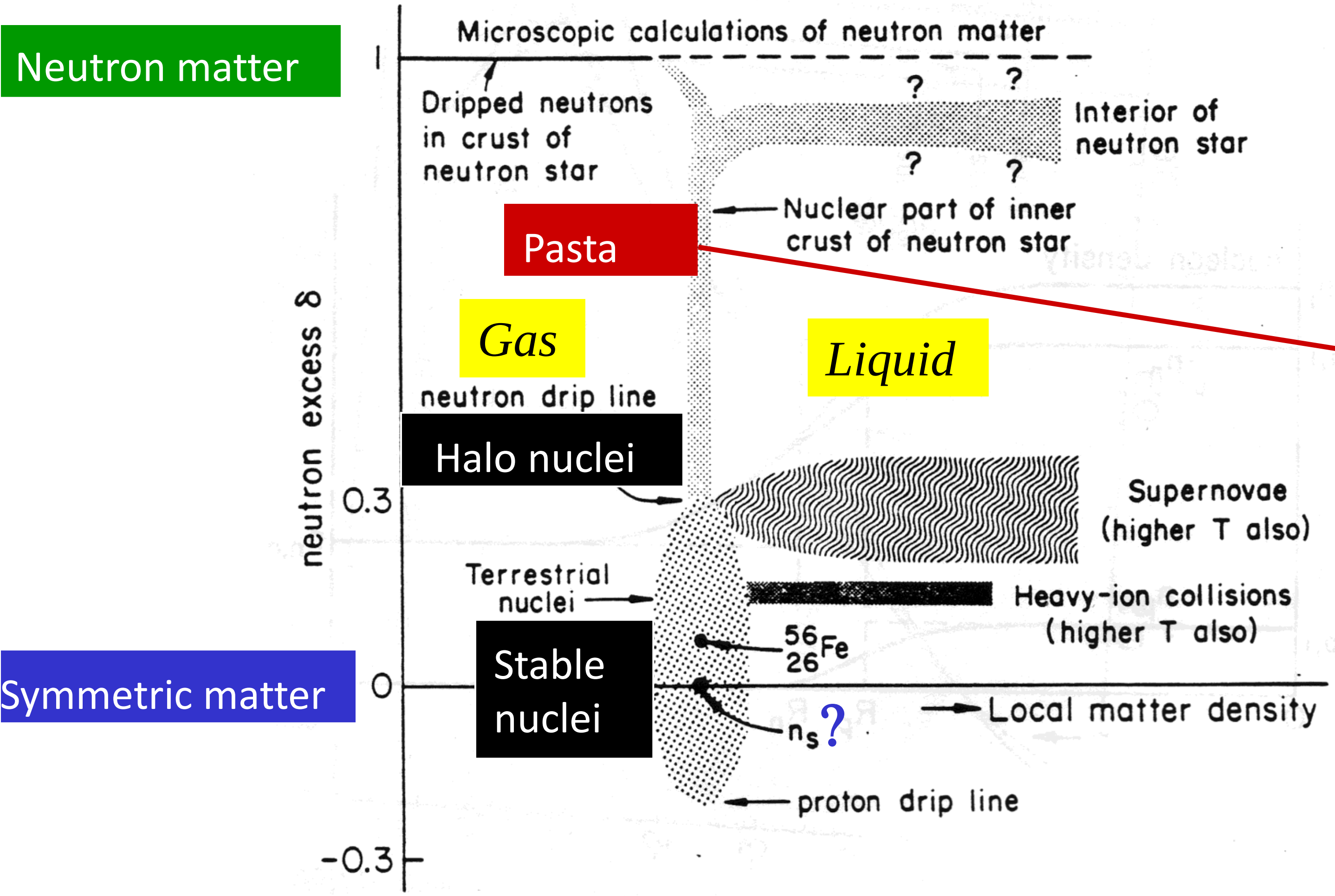

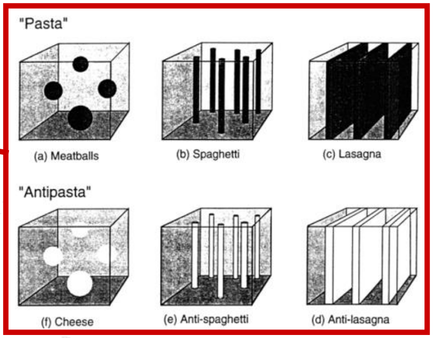

From Lamb (1991).

Pethick & Ravenhall, ARNPS **45** (1995) 429.

Microscopic EOS calculations

Pure neutron matter

Scattering length $a \approx -18$ fm
Effective range $R \approx 2$ fm

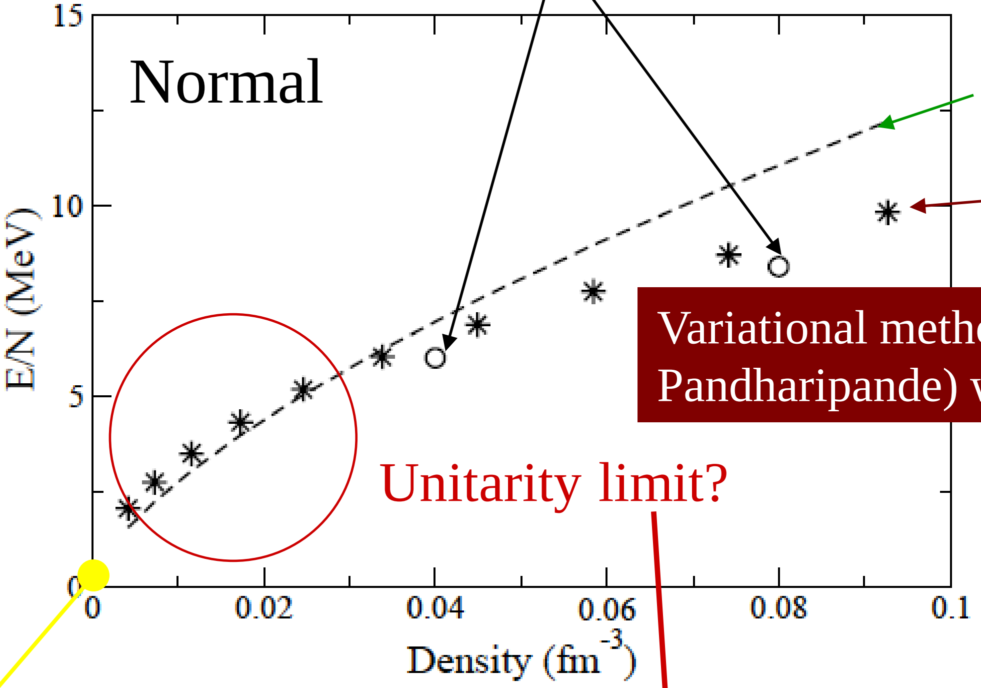

Green’s function Monte-Carlo (GFMC) with Argonne v_8’

$0.5E_{FG}/N$

Variational method (Friedman-Pandharipande) with Urbana v_{14}+TNI

Unitarity limit?

Low - density expansion :

$$E = E_{\mathrm{FG}}\left[1 + \frac{10}{9\pi}k_{\mathrm{F}}a + \frac{4}{21\pi^2}(11 - 2\ln 2)(k_{\mathrm{F}}a)^2 + \cdots\right]$$

Ref. Carlson et al., PRC **68** (2003) 025802.

$$|a| >> k_F^{-1} >> R$$

Microscopic EOS calculations (contd.)

Pure neutron matter

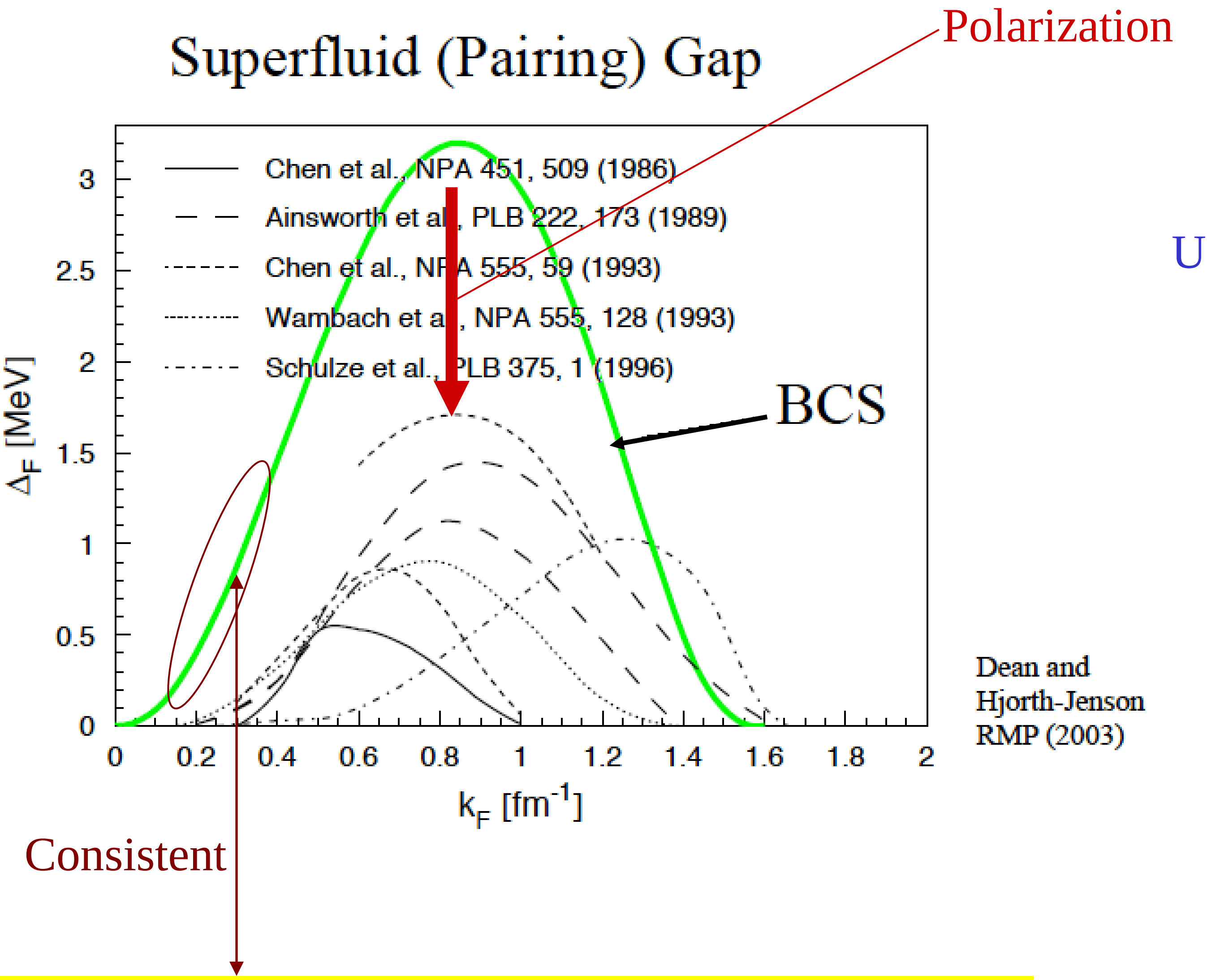

Dean and
Hjorth-Jenson
RMP (2003)

Uncertainties

large

↕

small

Unitarity limit (by QMC): $\Delta_F = 0.5(0.1) E_F$

Ref. Carlson and Reddy, PRL **95** (2005) 060401.

Phenomenological EOS parameters

Energy per nucleon of bulk nuclear matter near the saturation point (nucleon density *n*, neutron excess α):

$$w = w_0 + \frac{K_0}{18n_0^2}(n-n_0)^2 + \left[S_0 + \frac{L}{3n_0}(n-n_0)\right]\alpha^2$$

n_0, w_0	saturation density & energy of symmetric nuclear matter
S_0	symmetry energy coefficient
K_0	incompressibility
L	density symmetry coefficient

neutron

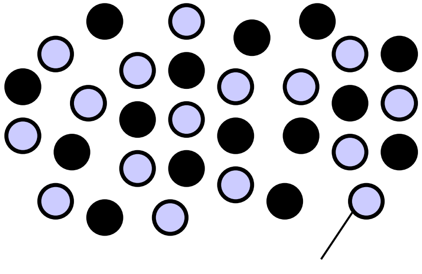

Proton with electric charge switched off

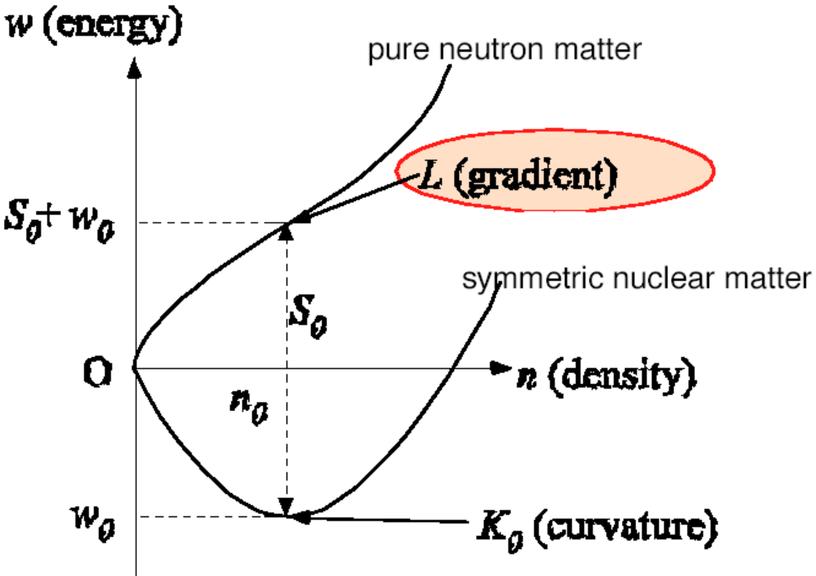

L is still uncertain, but controls various properties of neutron star crusts!

Phenomenological EOS parameters (contd.)

constraints on L

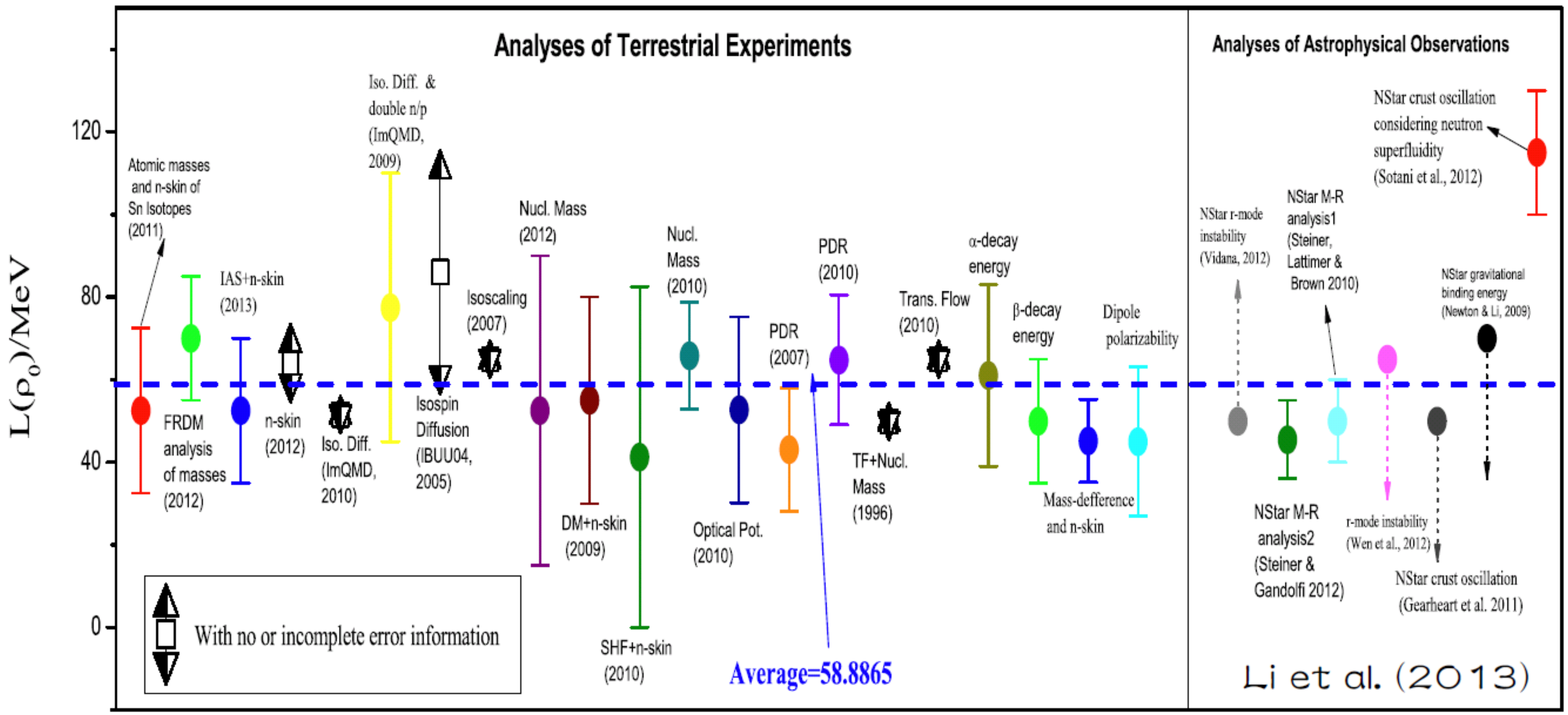

- most of constraints on L predict around $40 \lesssim L \lesssim 80$ MeV

Nuclear pasta as liquid crystals

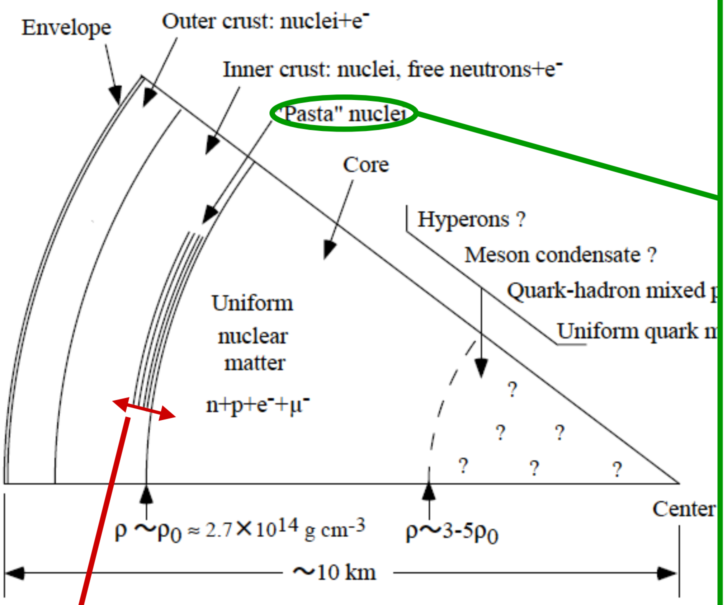

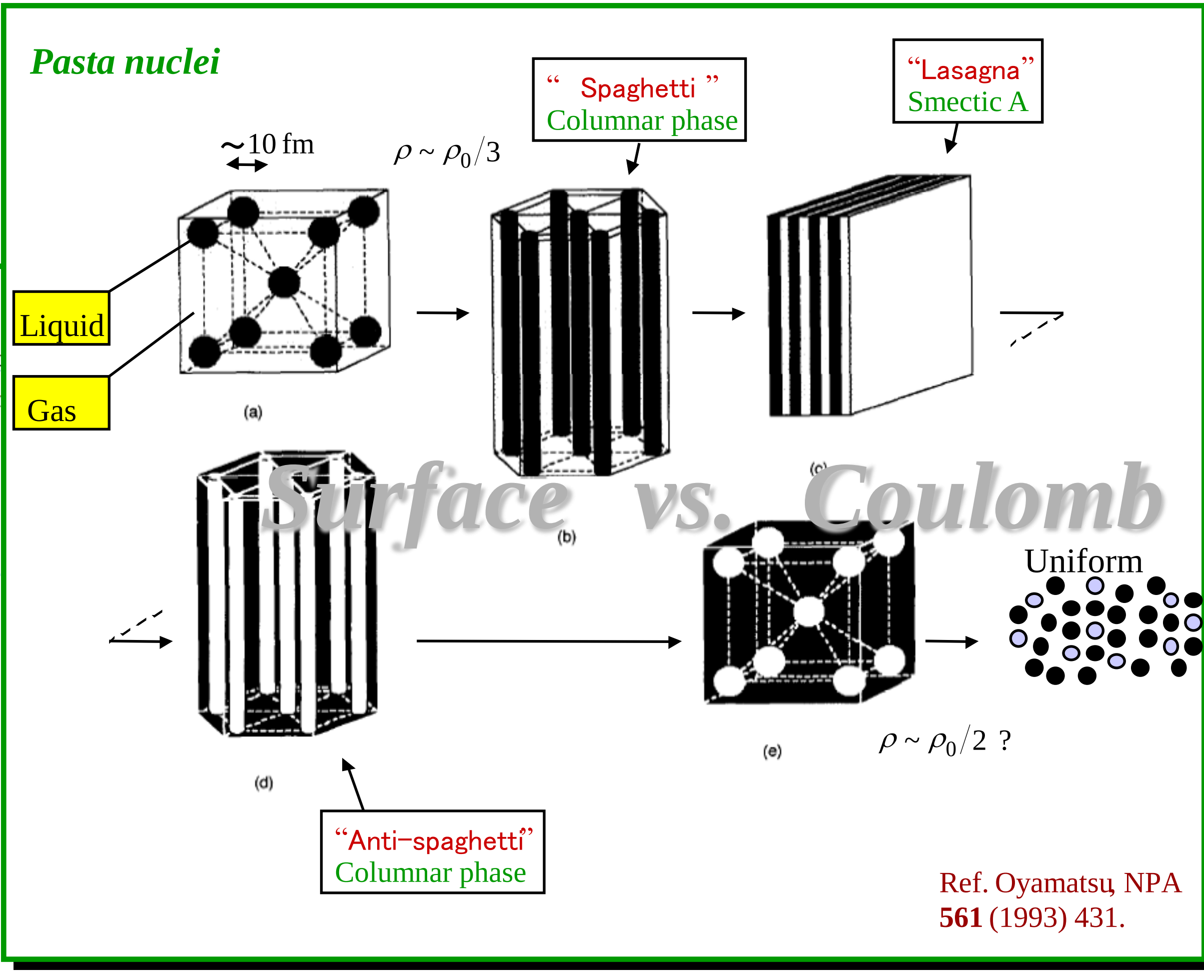

Surface vs. Coulomb

Ref. Oyamatsu, NPA **561** (1993) 431.

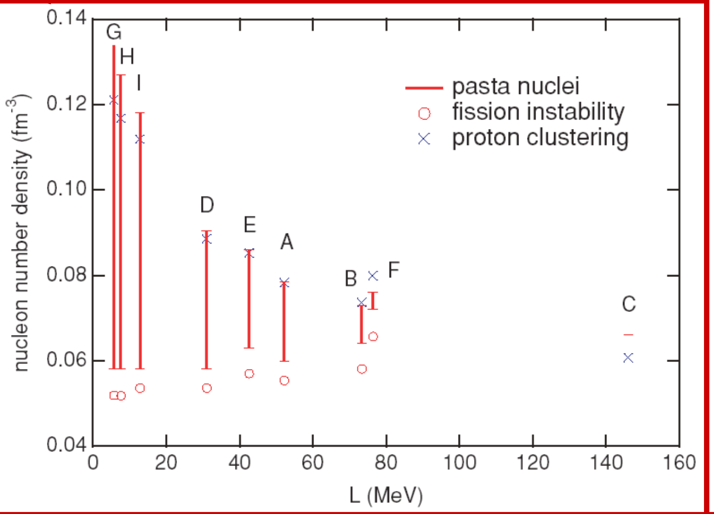

The larger *L*, the narrower pasta region.

Ref. Oyamatsu & Iida, PRC **75** (2007) 015801.

Pulsar glitch

From young pulsars, glitches, sudden decrease in the pulse period, are frequently observed.

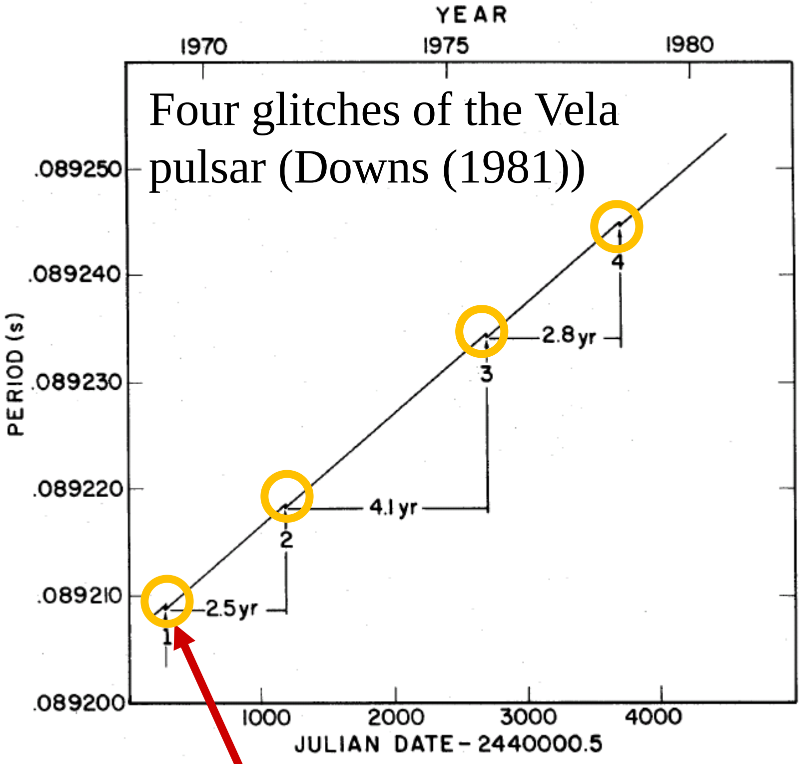

Four glitches of the Vela pulsar (Downs (1981))

Consistent with backreaction to disappearance of outwardly moving vortices, suggesting that superfluidity should occur in a neutron star!

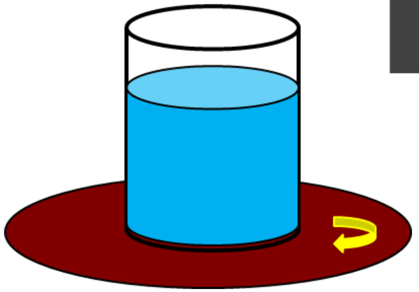

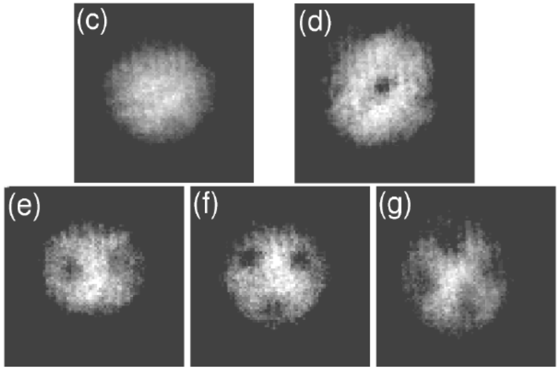

Vortices in rotating Bose condensate of Rb atoms (Madison et al.(2000))

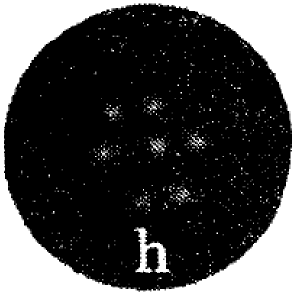

Vortices in rotating superfluid helium (Yarmchuk et al.(1979))

Charged component vs. neutron superfluid component

Superfluid component: $\mathbf{V}_n \cong \mathbf{\Omega}_n \times \mathbf{R}$ (uniform rotation) by a vortex lattice

Charged component: rotating with the pulsar frequency Ω ($< \Omega_n$)

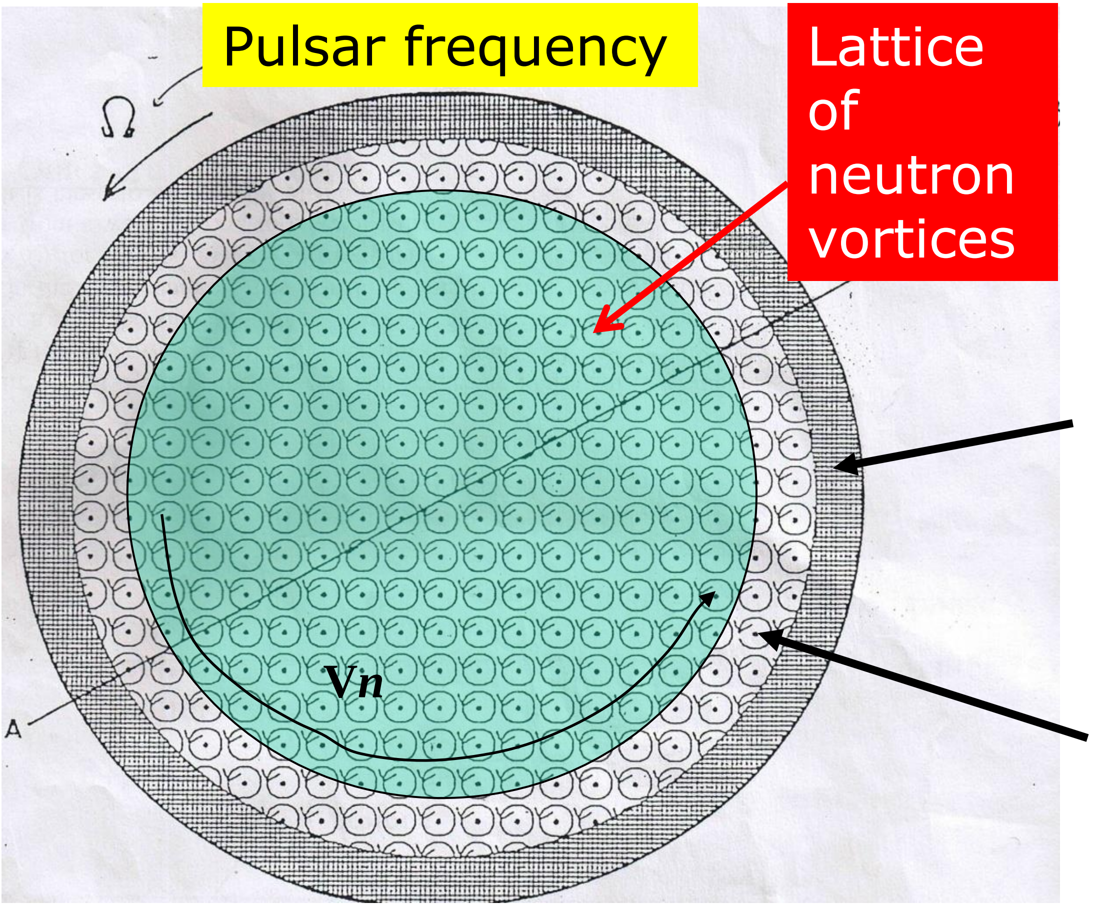

Pulsar frequency

Lattice of neutron vortices

Outer crust: charged component only

Inner crust: both components interact via vortex-nucleus coupling

Ref. J.A. Sauls (1989)

How to “brake” the neutron superfluid in the inter-glitch interval

The superfluid component has to slow down via coupling with a lattice of nuclei in the inter-glitch interval.

Conventional picture: drag on unpinned vortices (dissipative)

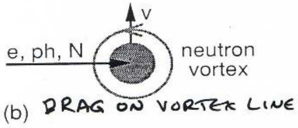

$I_n/I \sim 0.01$ (Vela)

Charged: $I_c\dot{\Omega} = -\alpha - \frac{I_c(\Omega-\Omega_n)}{\tau_c}$

Superfluid: $I_n\dot{\Omega}_n = \frac{I_c(\Omega-\Omega_n)}{\tau_c}$

Alternative picture: perfect pinning and entrainment effect (dissipationless)

Charged:

$$I_c\dot{\Omega} - \left(I_n - I_n^f\right)\left(\dot{\Omega} - \dot{\Omega}_n\right) = -\alpha$$

Superfluid:

$$\dot{J}_n = I_n\dot{\Omega}_n + \left(I_n - I_n^f\right)\left(\dot{\Omega} - \dot{\Omega}_n\right) = 0$$

Neutron band structure (pairing gap ignored)

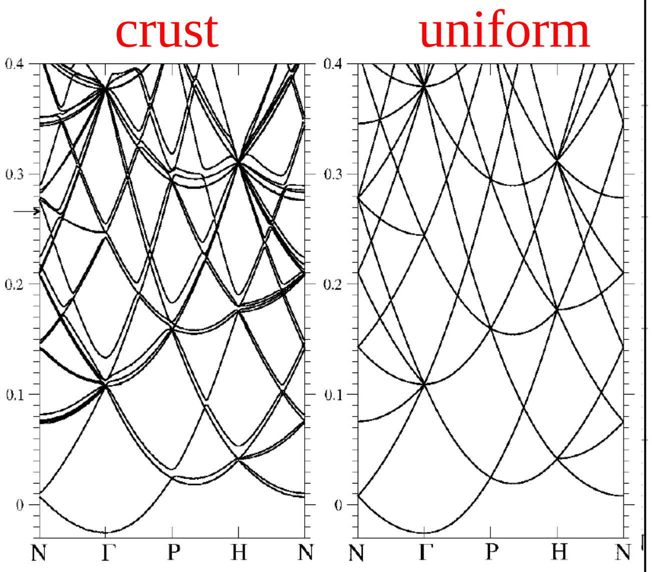

Chamel (2012).

A significant fraction of dripped neutrons is in filled bands and thus comoves with nuclei.

↓

Crust is not enough as a superfluid reservoir?

$I_n/I \sim 0.1$ (Vela)

Caveat: Bragg scattering suppressed for quasiparticles (ph superpositions)

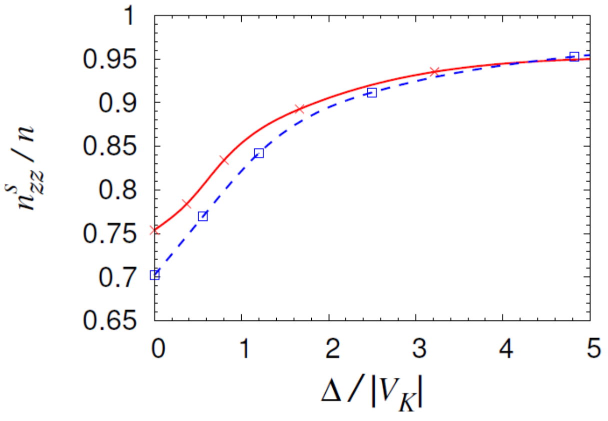

Watanabe & Pethick (2017).

How a neutron vortex is pinned in a crust?

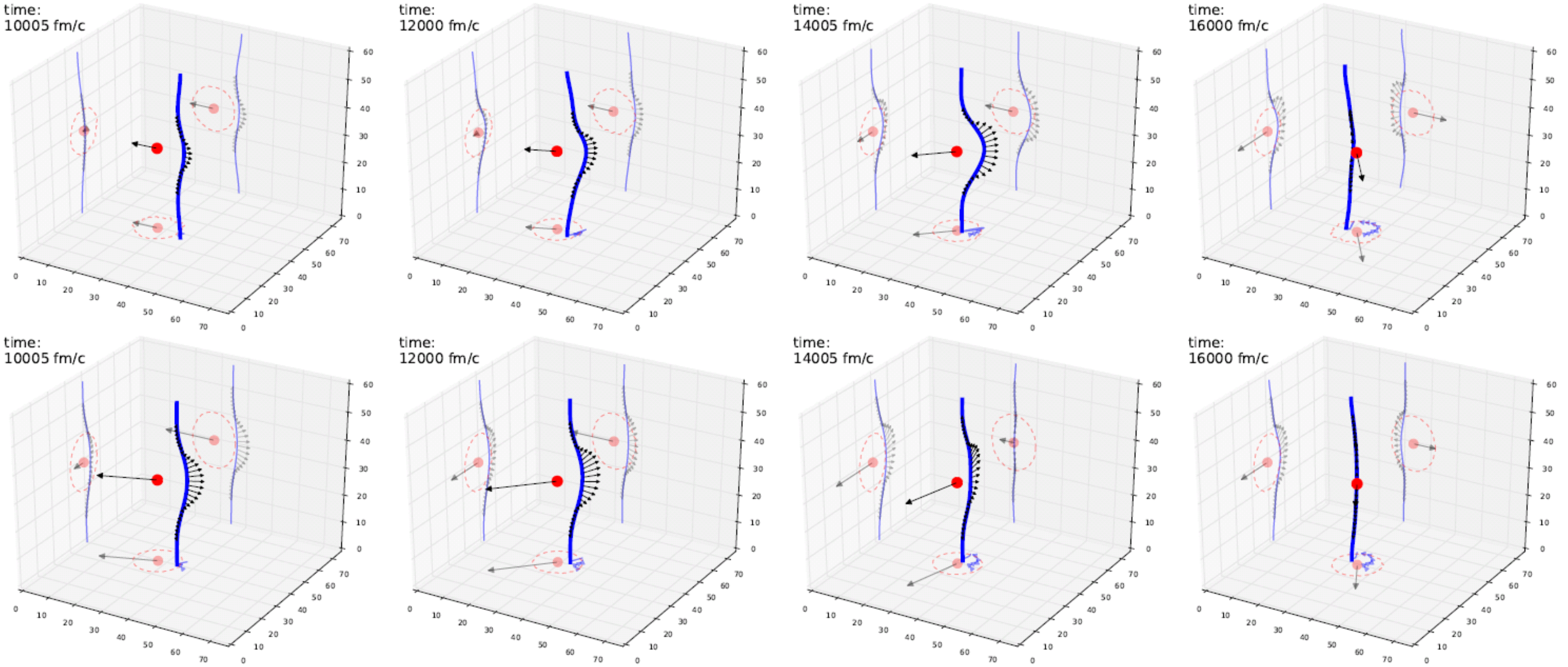

FIG. 2. (Color online) Dynamics of the system for times corresponding to small vortex-nucleus separations for neutron matter density $n = 0.014\ \mathrm{fm}^{-3}$ (top) and $0.031\ \mathrm{fm}^{-3}$ (bottom). Frames from left to right correspond to times $(10, 12, 14, 16) \times 1{,}000\ \mathrm{fm}/c$ (for full movies see [16]). Blue line indicates the vortex core position extracted from the order parameter Δ (see [16] for details). Red dot indicates position of the center of mass of protons. The vector attached to the red dot denotes the vortex-nucleus force $\boldsymbol{F}(R)$. Vectors attached to the vortex indicate contributions to the force $-d\boldsymbol{F}$ extracted from force per unit length, see Eq. (3) and inset (a) of Fig. 3. They are scaled by factor 3 for better visibility. Projections of the view are shown on sides of the box. Red dashed lines denote shape of nucleus (defined as a point where density of protons drops to value $0.005\ \mathrm{fm}^{-3}$). By blue triangles (on XY-plane) trajectory of the vortex up to given time is shown.

Ref. Wlazłowski, Sekizawa et al., PRL 117 (2016) 232701 (2016)

QPOs in giant flares from soft-gamma repeaters (SGRs)

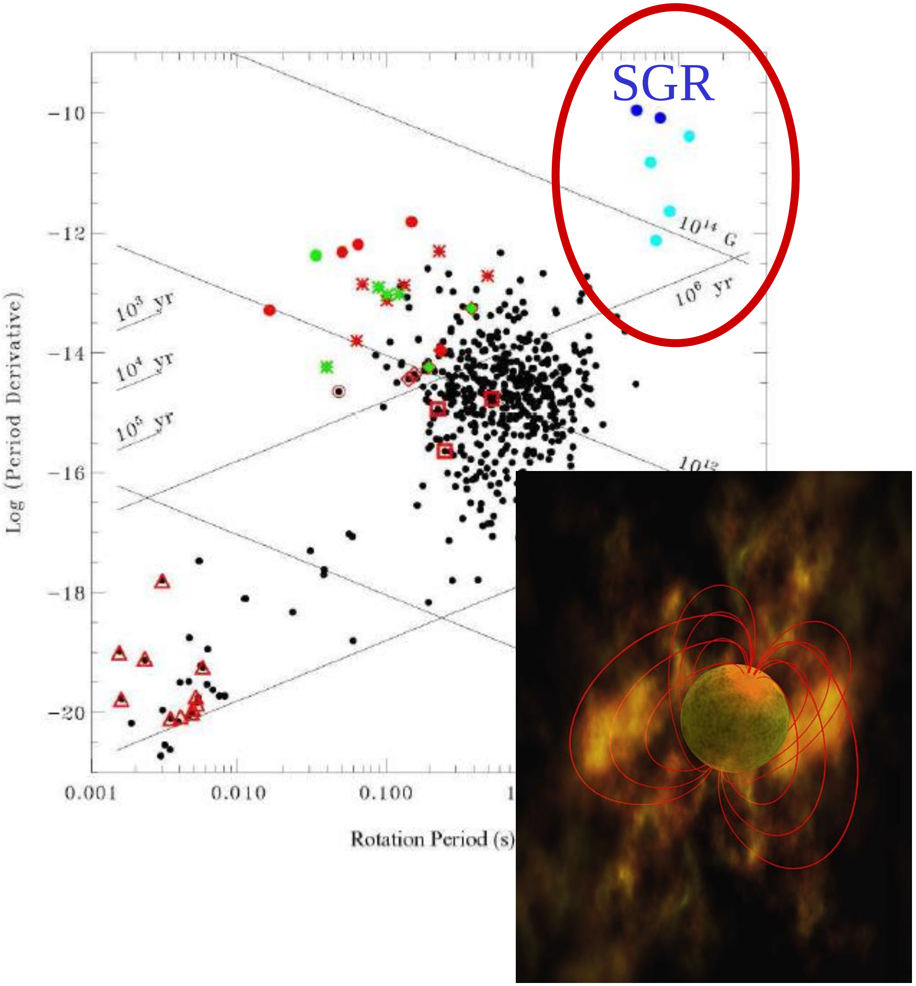

arXiv:astro-ph/0208356

image
by NASA

X-ray light curve of the SGR 1806-20 giant flare

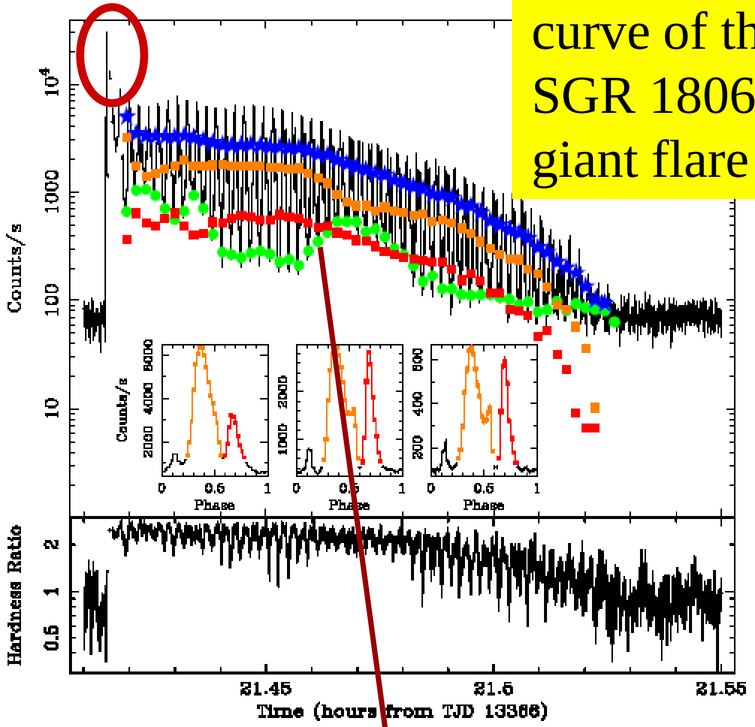

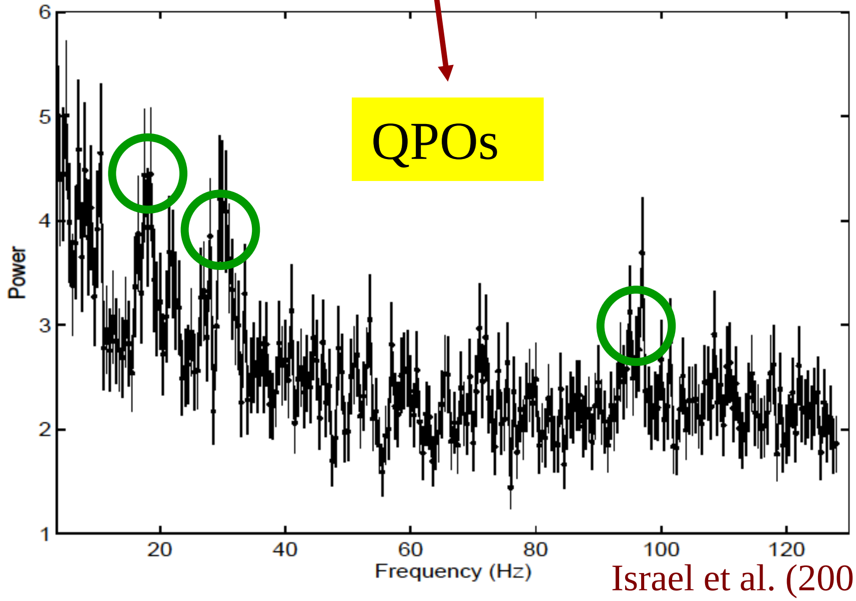

Israel et al. (2005)

QPOs in giant flares from SGRs (contd.)

X-ray light curve of the SGR 1806-20 giant flare

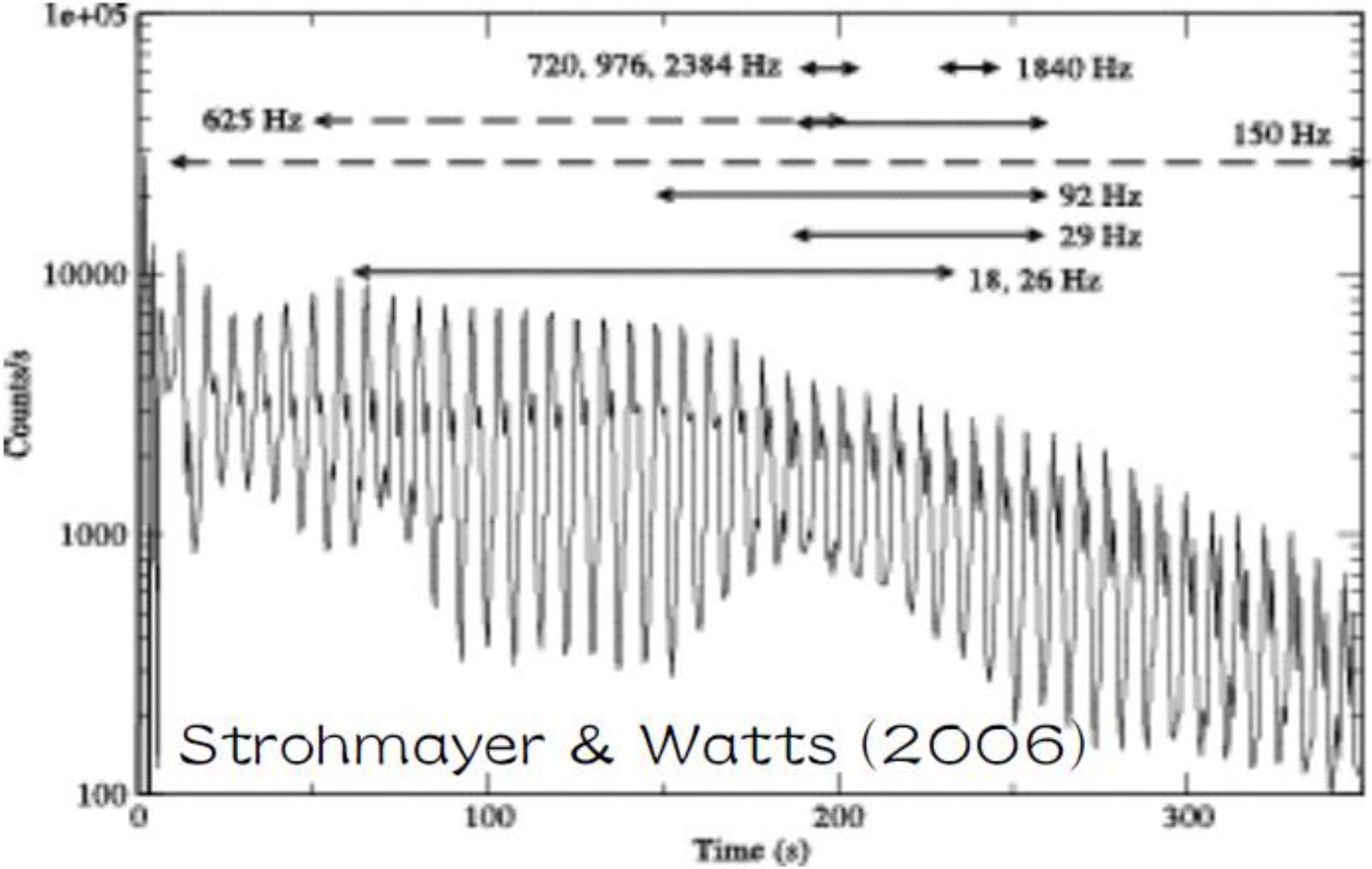

Strohmayer & Watts (2006)

QPOs in giant flares from SGRs (contd.)

Possible identification of the observed QPOs as manifestations of global torsional shear oscillations in a neutron star crust

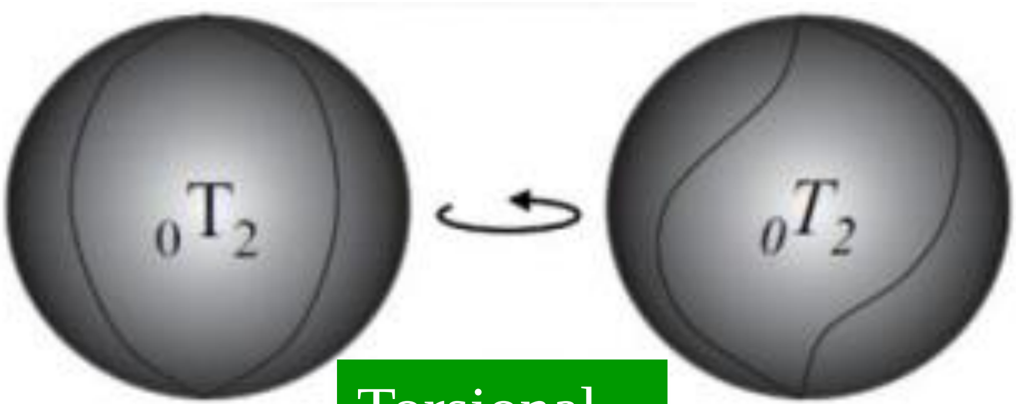

Torsional oscillations

From Heki.

Shear modulus $\propto Z^2$

↓

Possible constraint on L

Equilibrium nuclear size in the inner crust of a neutron star

Ref. Oyamatsu & Iida, PRC **75** (2007) 015801.

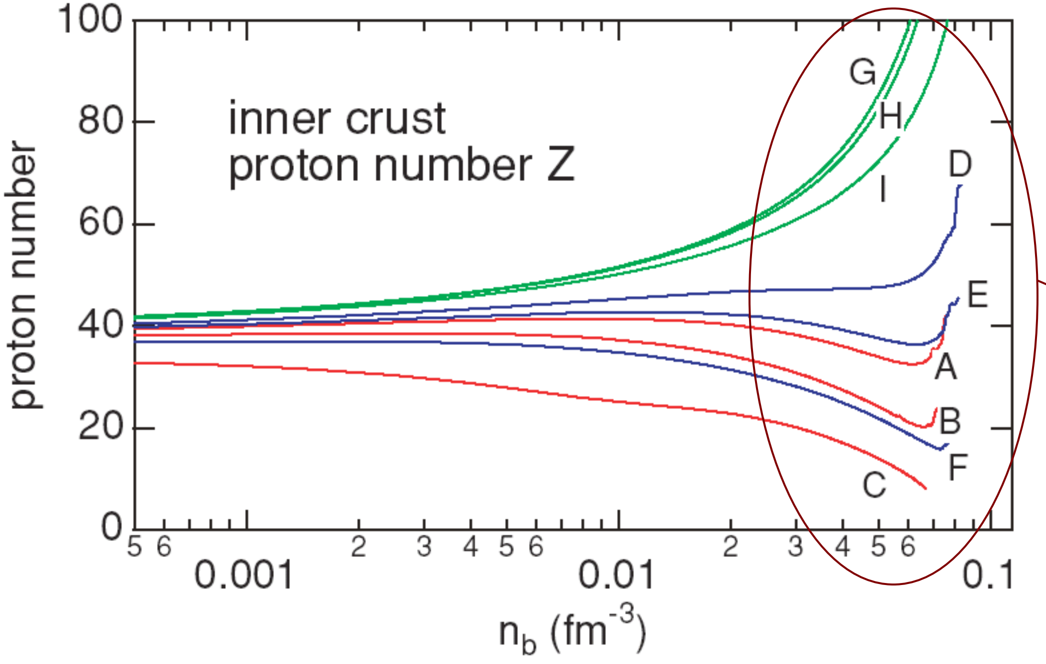

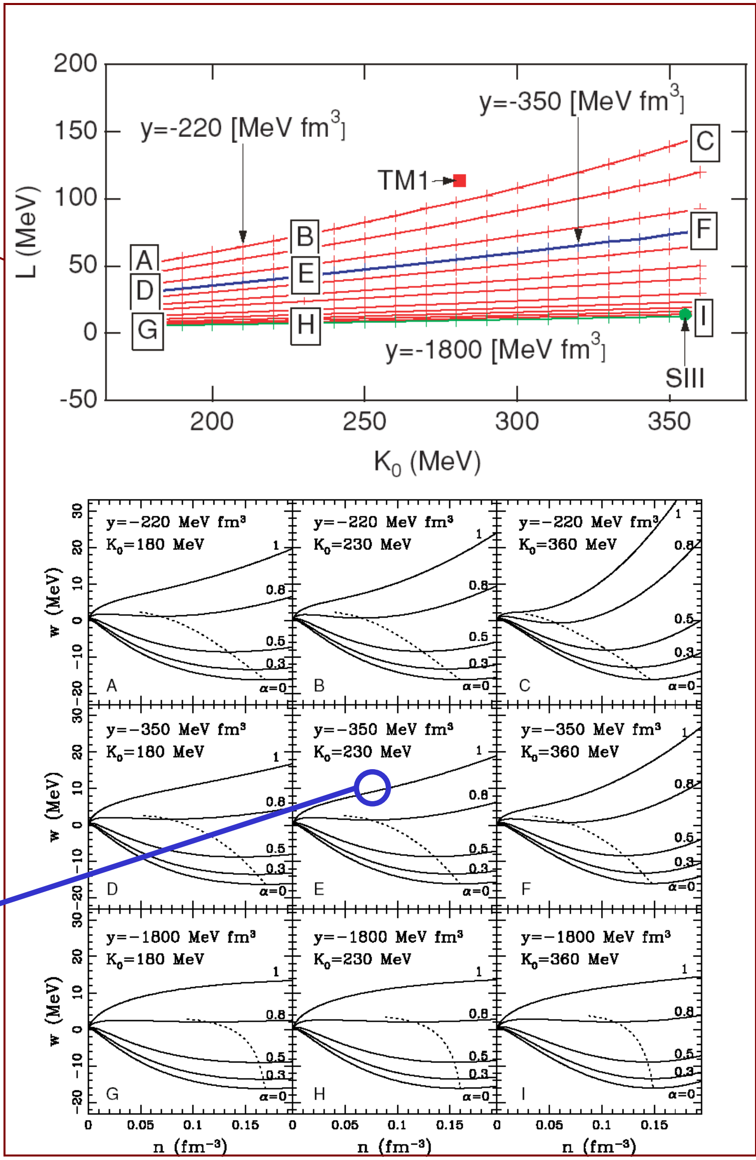

The larger *L*, the smaller size.

close to the GFMC result
with the Argonne v_8' potential

Constraint on *L* from crustal torsional oscillation frequencies

Ref. Sotani, Nakazato, Iida, & Oyamatsu, arXiv:1202.6242.

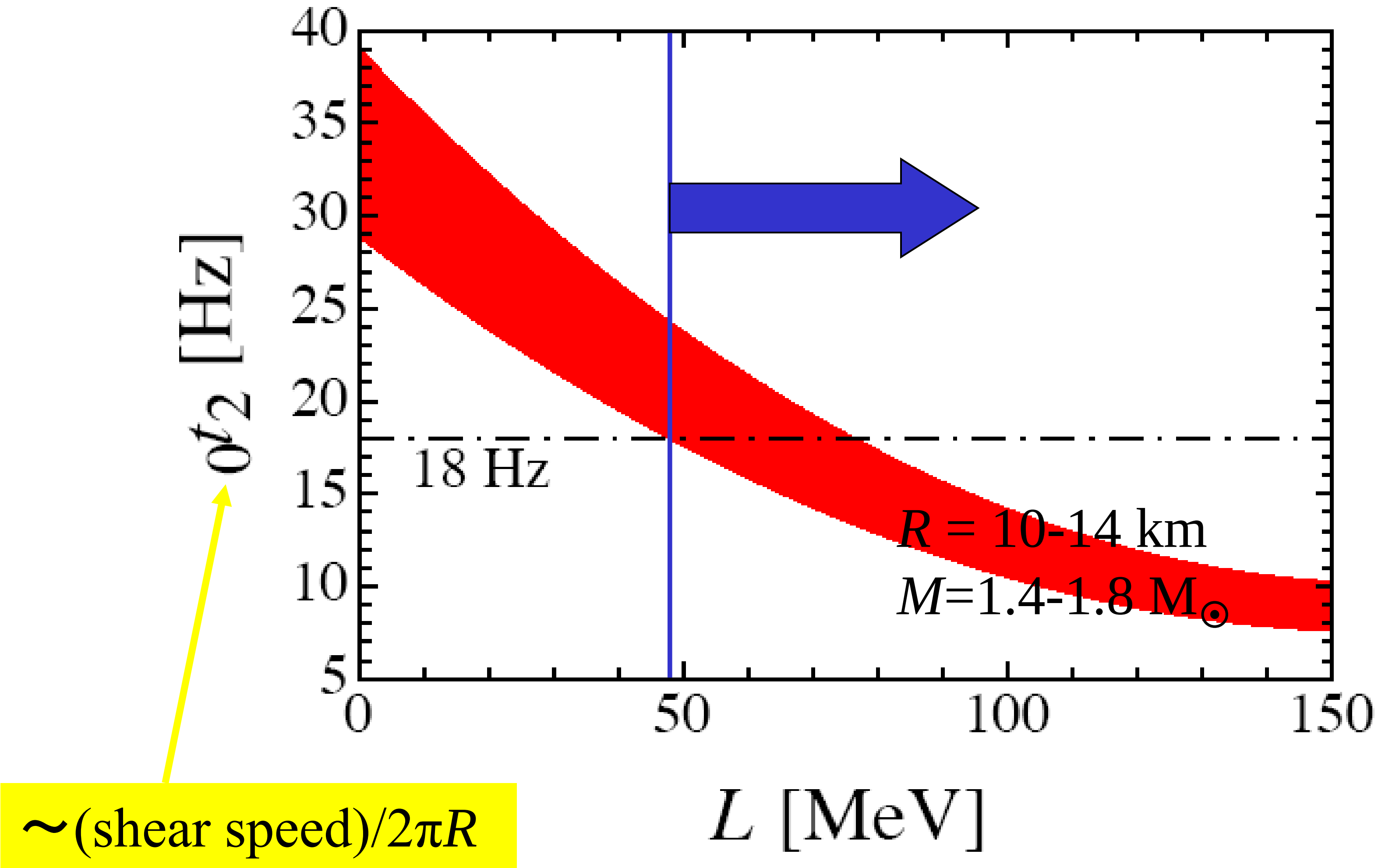

∼(shear speed)/2πR

Effects of superfluidity on crustal oscillations

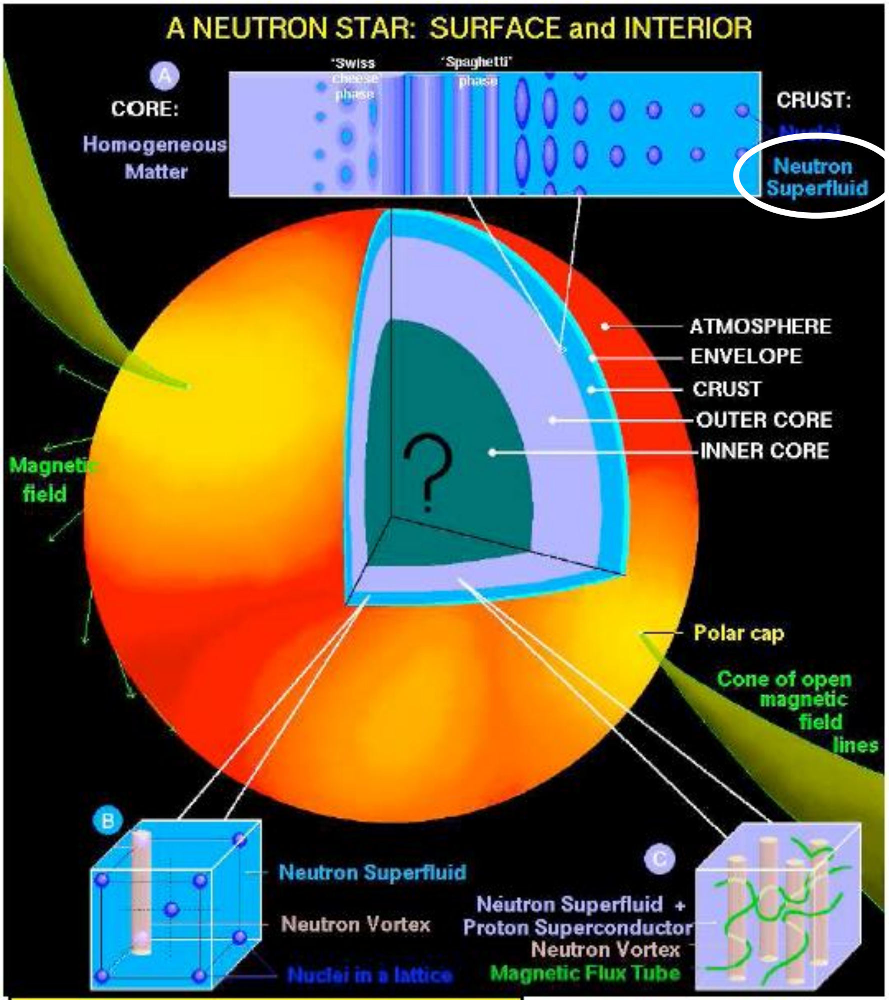

Lattimer and Prakash, astro-ph0405262

Figure by D. Page

Neutron band structure

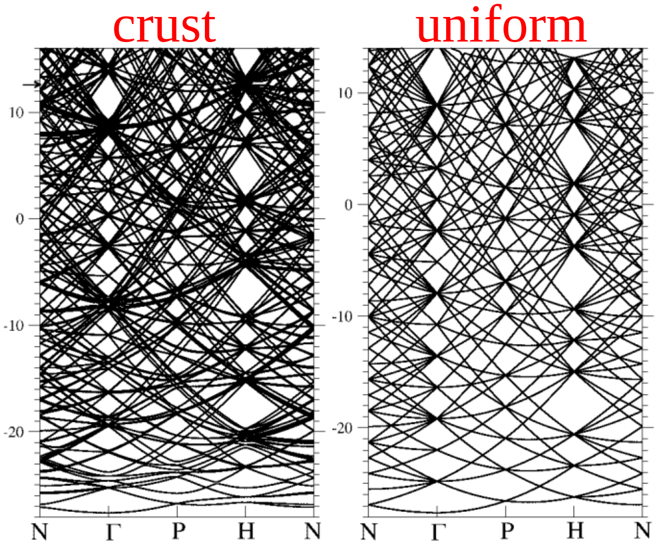

Chamel (2012).

Torsional oscillation frequency

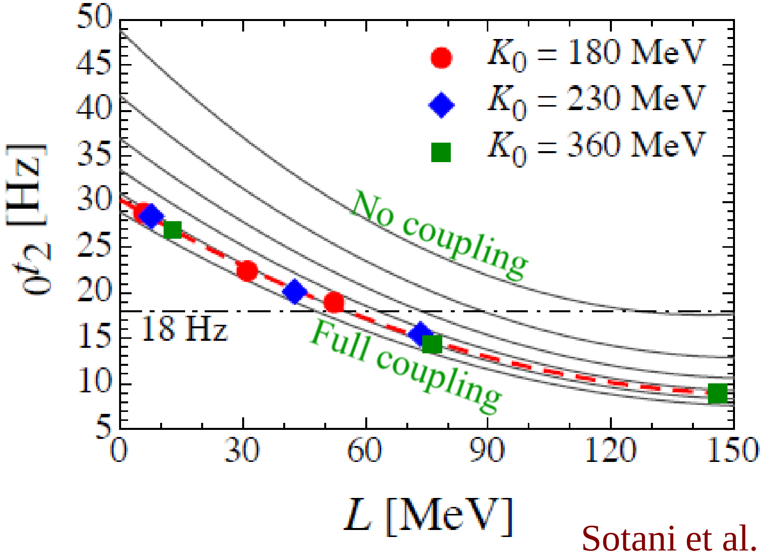

Sotani et al. (2012).

Superfluid neutrons are coupled with a lattice of nuclei.

Neutron matter and trapped cold atoms

Low density neutron matter

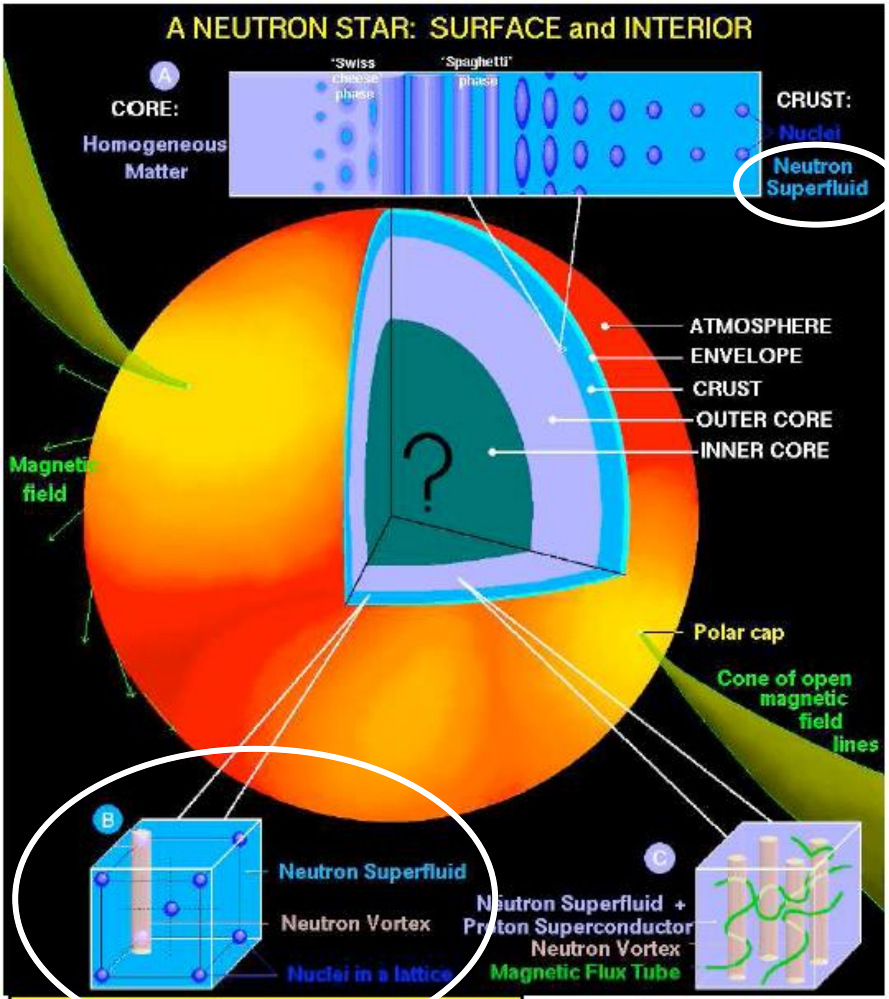

Lattimer and Prakash, astro-ph0405262

Figure by D. Page

Cold Fermi atoms near Feshbach resonance

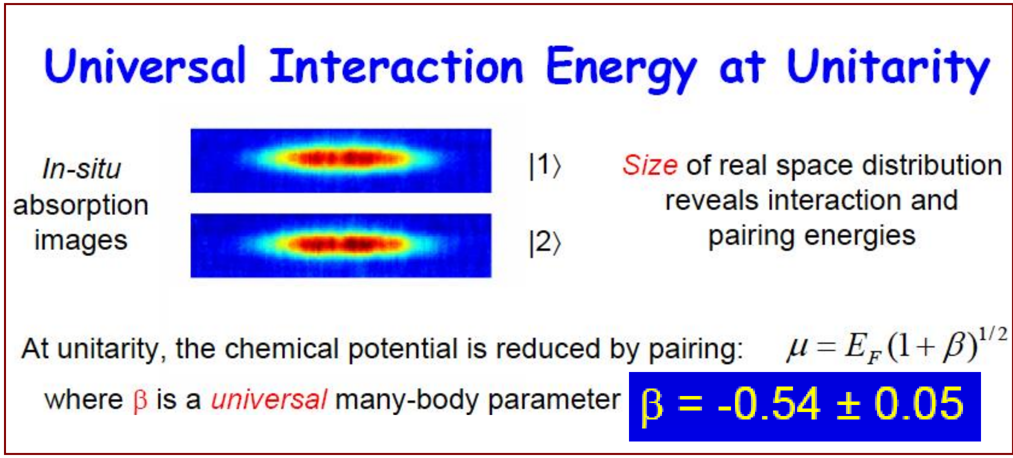

Universal Interaction Energy at Unitarity

In-situ absorption images

|1⟩

|2⟩

Size of real space distribution reveals interaction and pairing energies

At unitarity, the chemical potential is reduced by pairing: $\mu = E_F(1+\beta)^{1/2}$

where β is a *universal* many-body parameter $\beta = -0.54 \pm 0.05$

From R. Hulet.

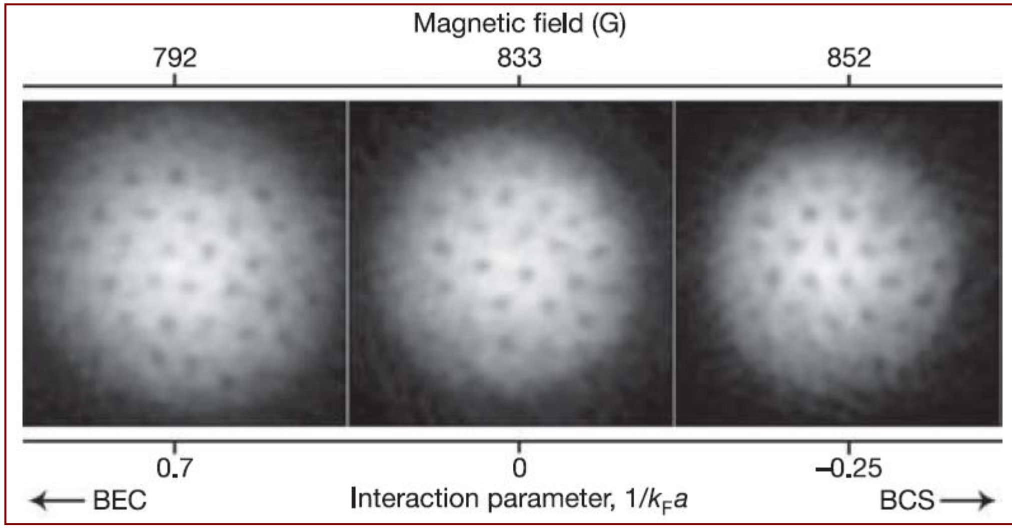

From M.W. Zwierlein.

Few alpha systems in dilute neutron matter

Possible binding

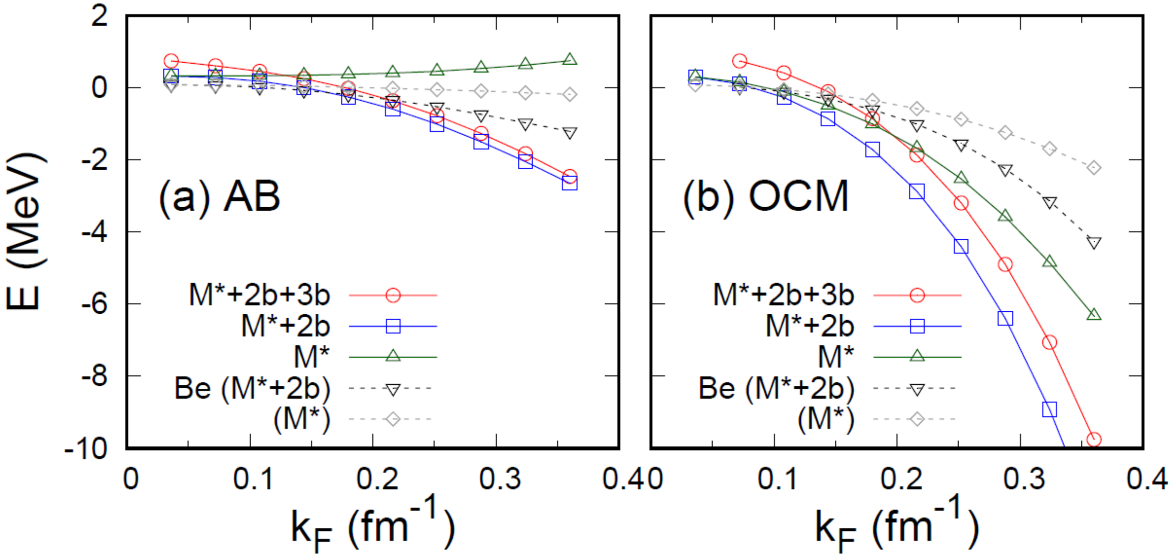

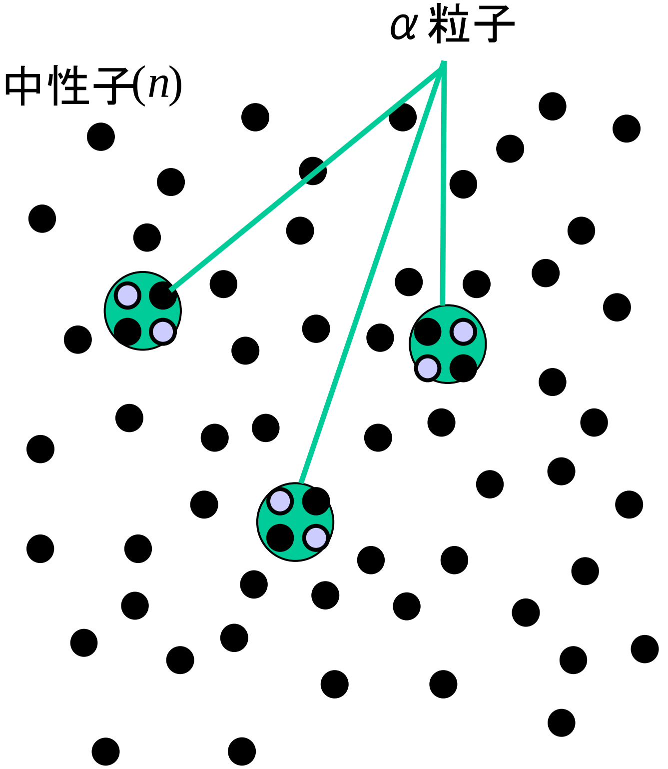

$$H = \sum_{i=1}^{3} \frac{p_i^2}{2M^*} - T_{\rm cm} + \sum_{i<j=1}^{3} \left[U_{ij}^{(2)} + V_{{\rm eff};ij}^{(2)} \right] + U^{(3)} + V_{\rm eff}^{(3)}$$

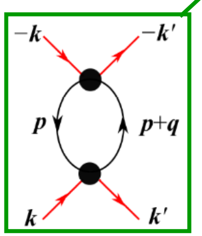

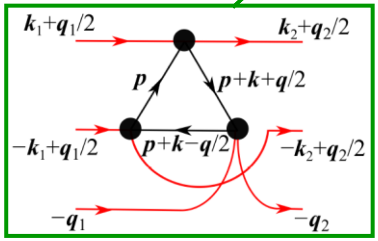

H. Moriya et al., arXiv:2106.14469.

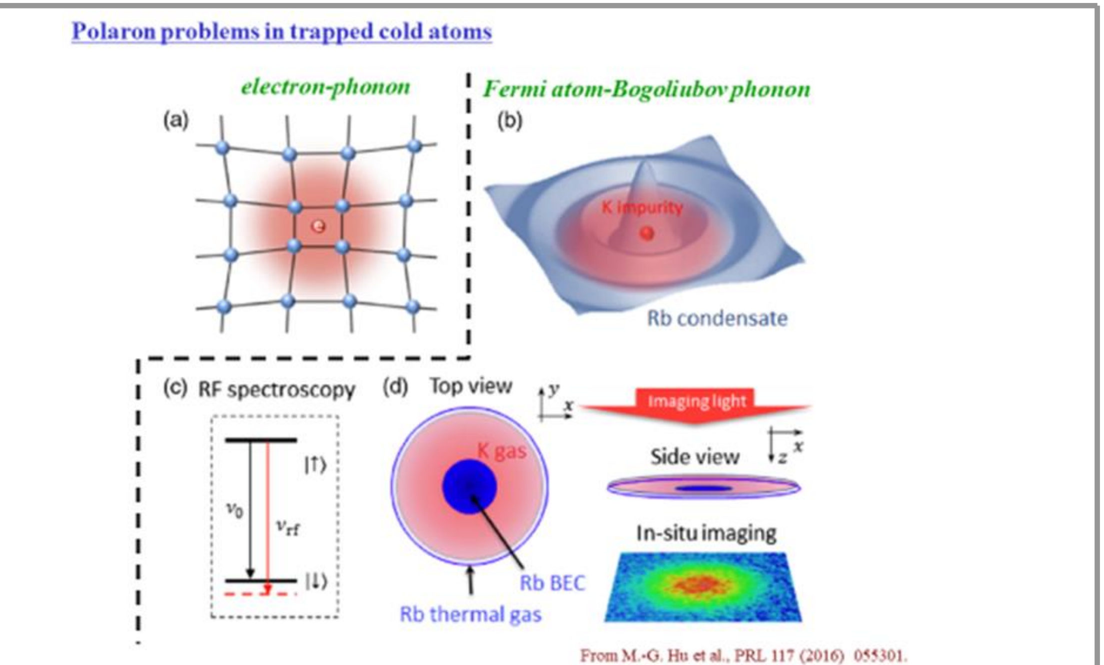

Polaron problems in trapped cold atoms

From M.-G. Hu et al., PRL 117 (2016) 055301.

Possible emergence of Cooper triples in quark matter

By Fukushima

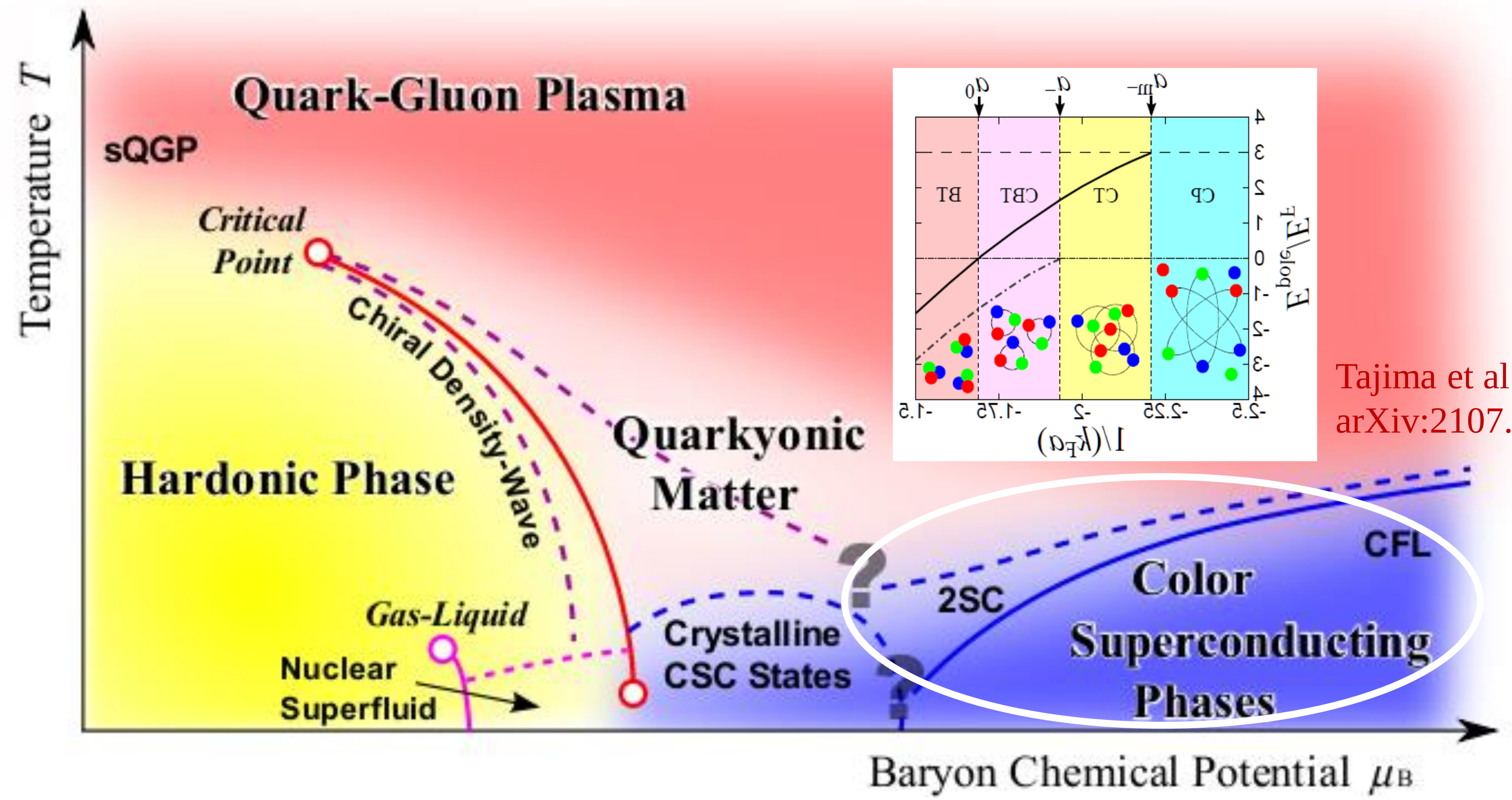

Tajima et al.,
arXiv:2107.13232

$|RGB\rangle$

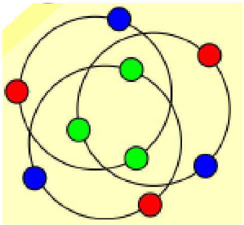

vs.

$|RG\rangle - |GR\rangle, |GB\rangle - |BG\rangle, |BR\rangle - |RB\rangle$

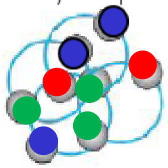

Condensate of "Cooper triples"
Ref. Akagami, Tajima, & Iida (2021)

Color-flavor locked condensate of "Cooper pairs"
Ref. Alford, Rajagopal, & Wilczek (1999)

A3 foresight program: Various Manifestations of Nuclear Structure --------- From Nucleons to Nuclear Matter at Extreme Conditions

Working group: G. Watanabe, Y. Minami (Zhejiang), T. Nakatsukasa (Tsukuba), M. Matsuo, T. Sasaki (Niigata), K. Sekizawa (TIT), K. Iida (Kochi)…

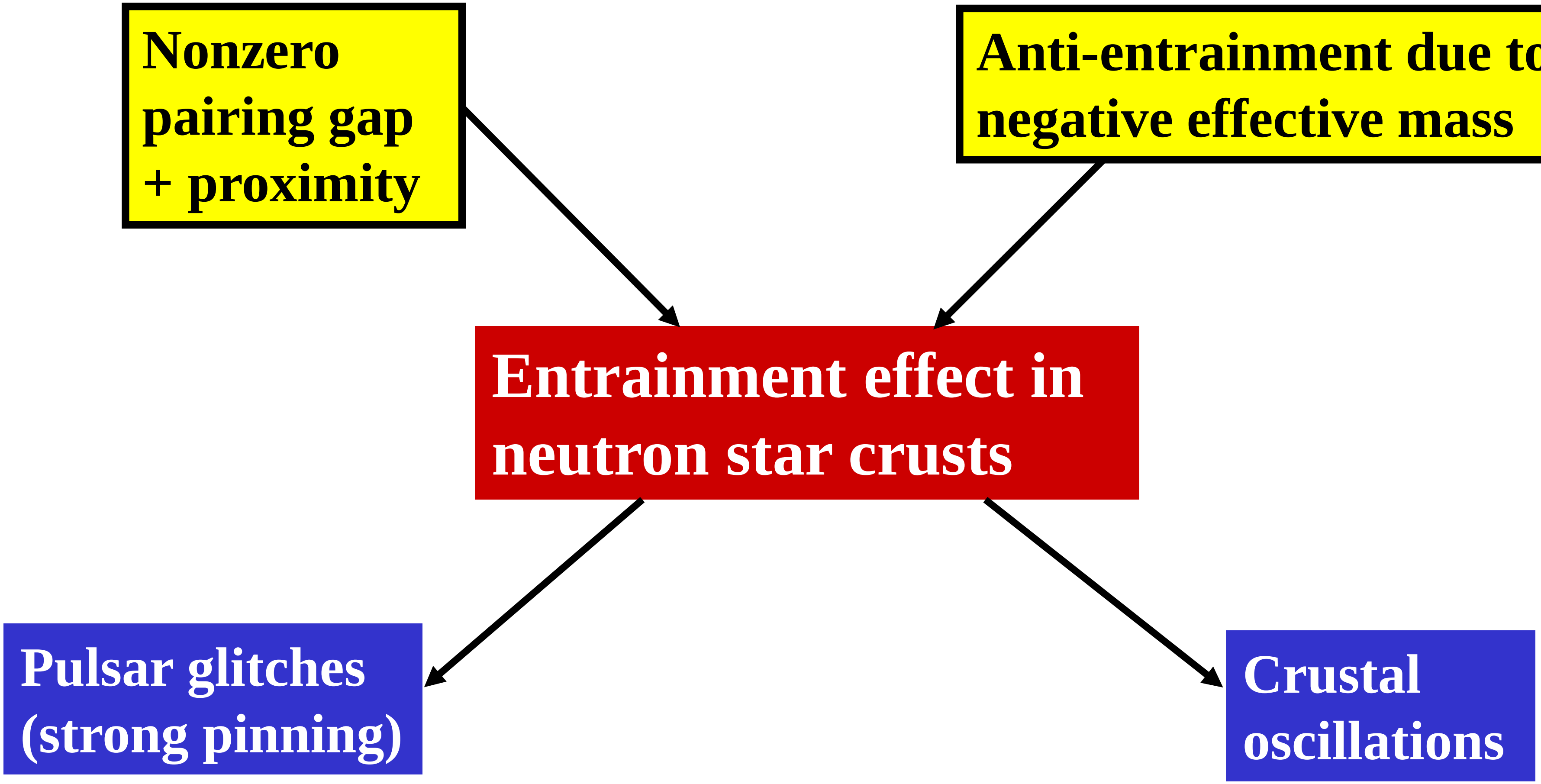

Nonzero pairing gap + proximity

Anti-entrainment due to negative effective mass

Entrainment effect in neutron star crusts

Pulsar glitches (strong pinning)

Crustal oscillations

Anti-entrainment due to negative effective mass

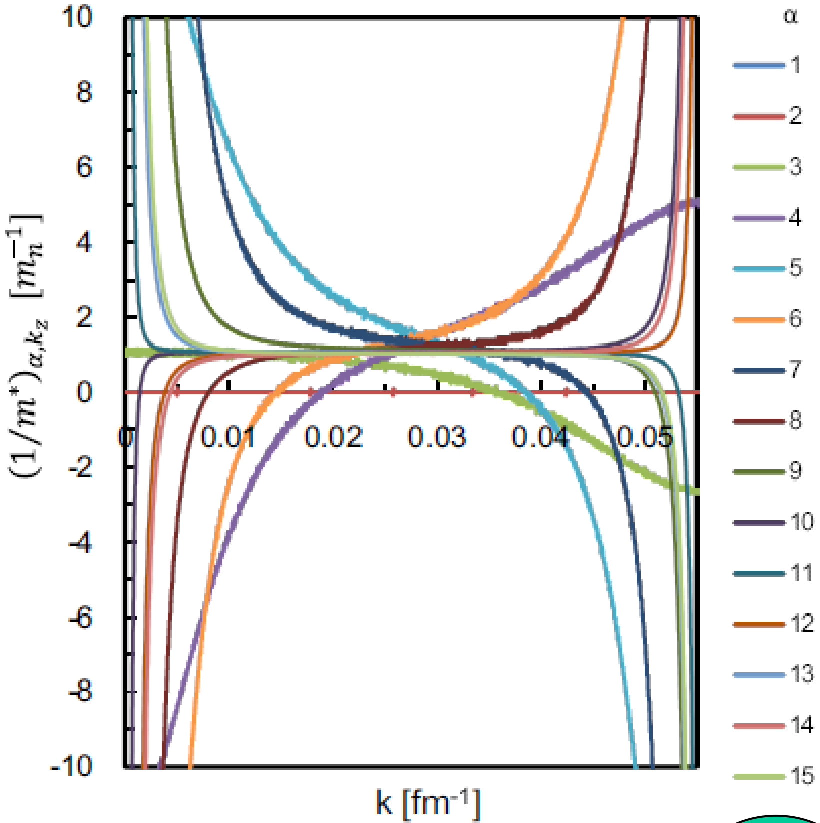

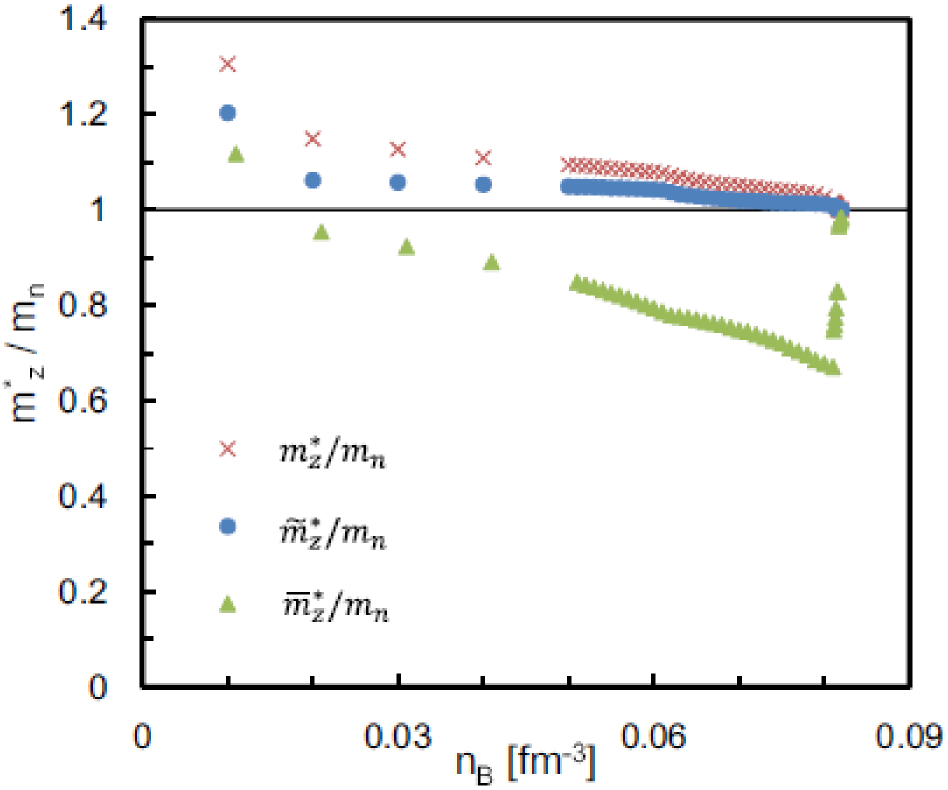

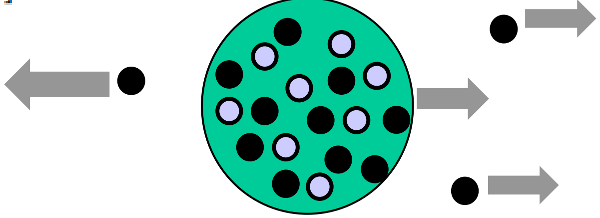

Kashiwaba & Nakatsukasa (2019).

Nonzero pairing gap + proximity

Realistic Wigner-Seitz cell R_{cell} vs $R_{\mathrm{edge}} + \xi$

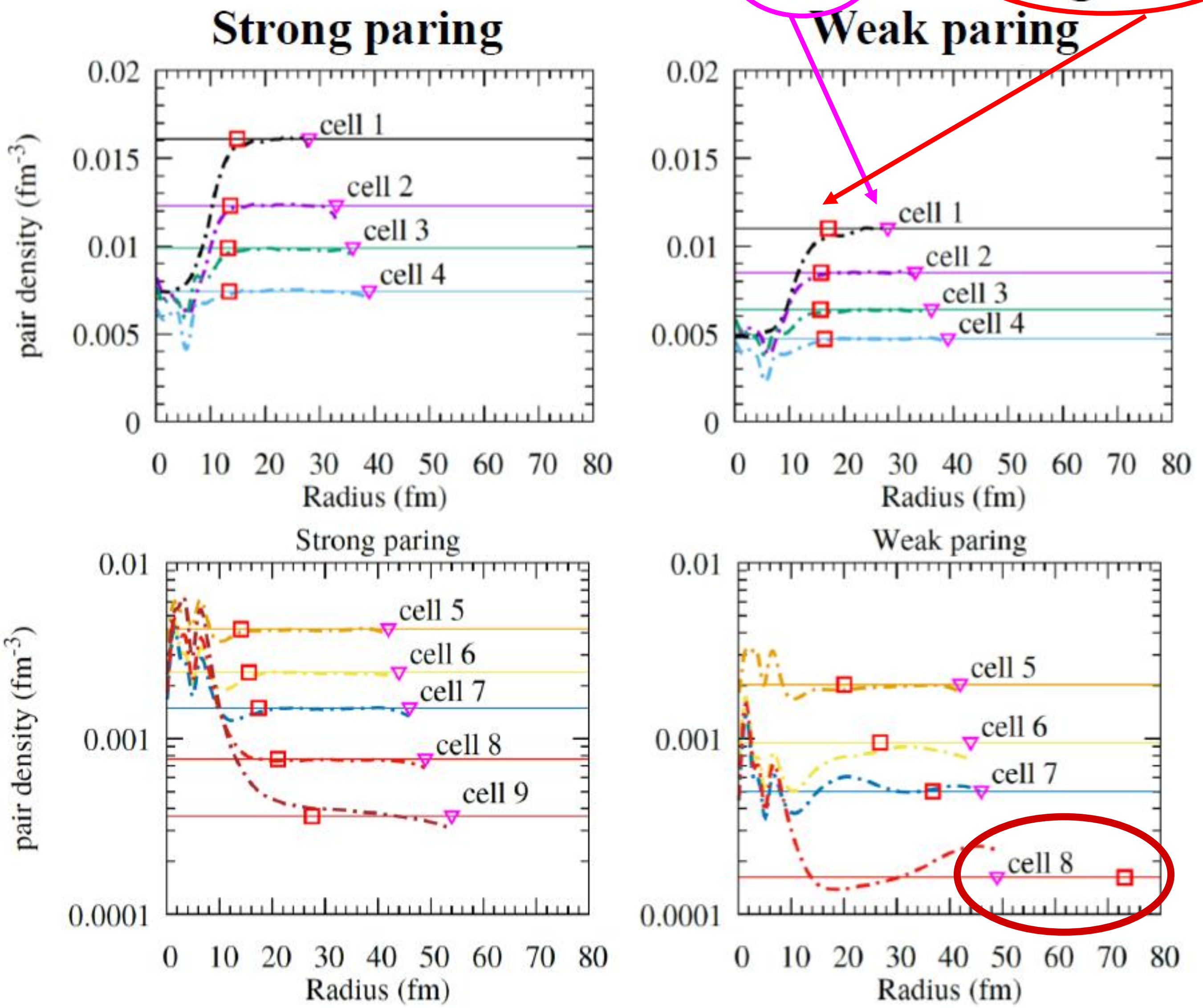

Okihashi & Matsuo (2019).

Amorphous effects on the superfluid density

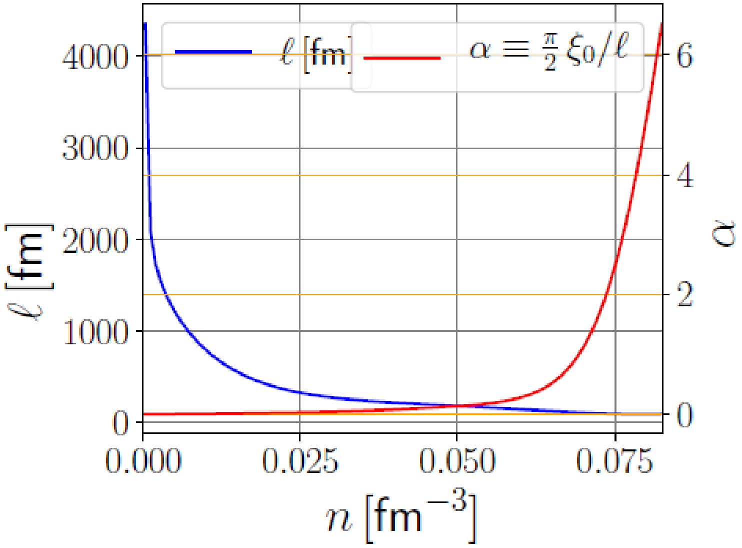

FIG. 1. The transport *mfp*, ℓ, for neutrons in an amorphous nuclear solid crust is shown with the blue line as a function of neutron density. The *mfp* varies from $\ell_{\text{max}} = 4360\,\text{fm}$ at low density to $\ell_{\text{min}} = 80\,\text{fm}$ at high density. The corresponding pair-breaking parameter, $\alpha = \frac{\pi}{2}\xi_0/\ell$, is shown as the red line.

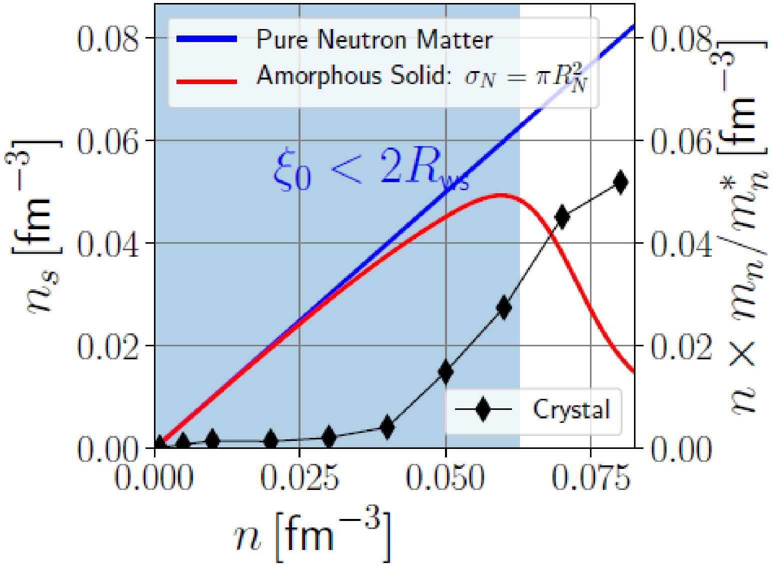

FIG. 2. Suppression of the zero-temperature neutron superfluid density in an amorphous crust (red line). The blue line, $n_s = n$, is for pure neutron matter at $T = 0$. The prediction from Ref. 19 of the conducting neutron density, $n_c = n \times m_n/m_n^*$, obtained from the band effective mass ratio for a bcc crystal of nuclei, is shown with black diamonds. The shaded region is where the pure neutron superfluid coherence length is *less* than the distance between nuclei.

Sauls, Chamel, & Alpar (2020).

More on magnetar QPOs: Bayesian QPO analysis and "lasagna-sandwich" model

Ref. Sotani et al., arXiv:1906.06999.

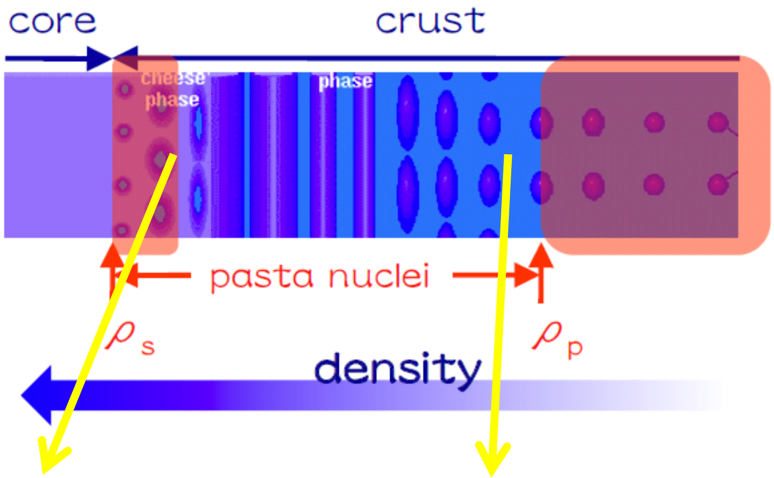

bubble＋tube (lasagna) sphere+rod

${}_0t_2$～(shear speed)/$2\pi R$

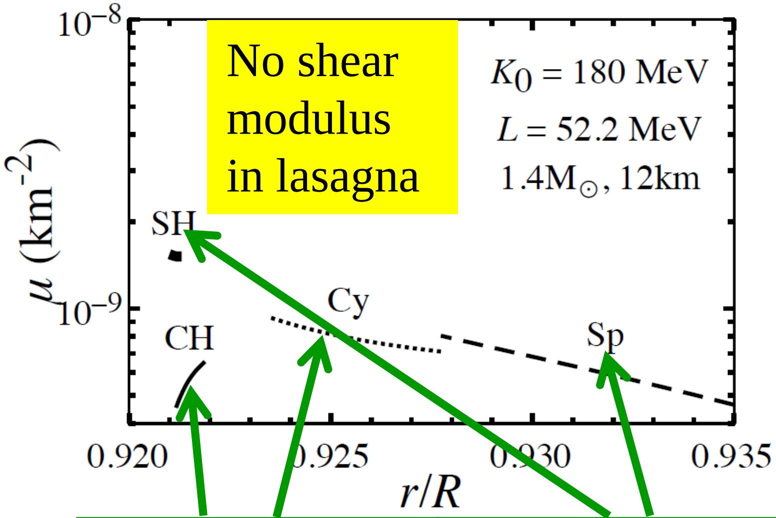

No shear modulus in lasagna

Rod: Pethick & Potekhin (1998)

Sphere: Ogata & Ichimaru (1990)

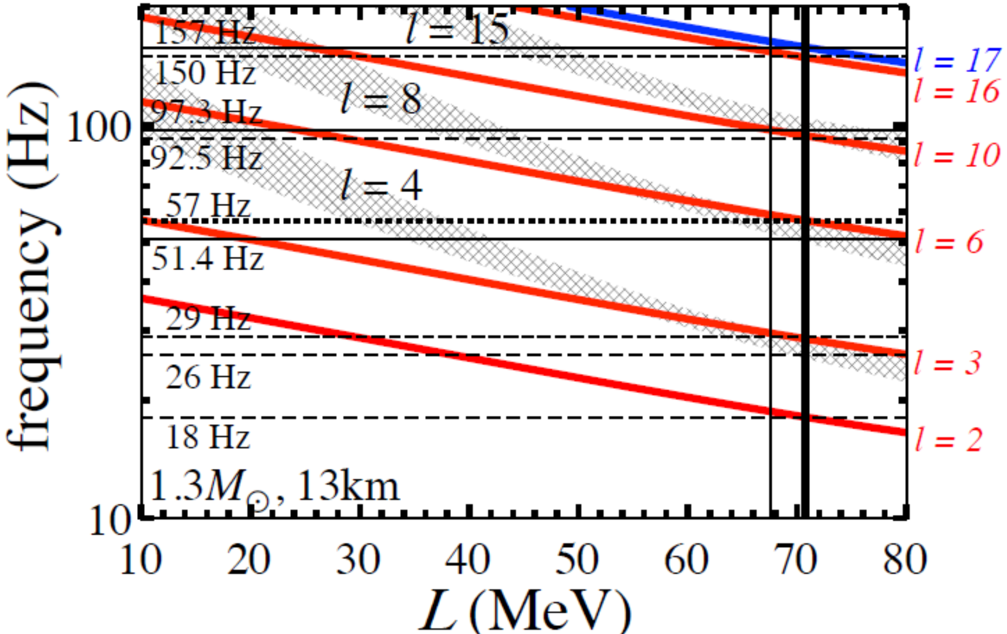

vs.

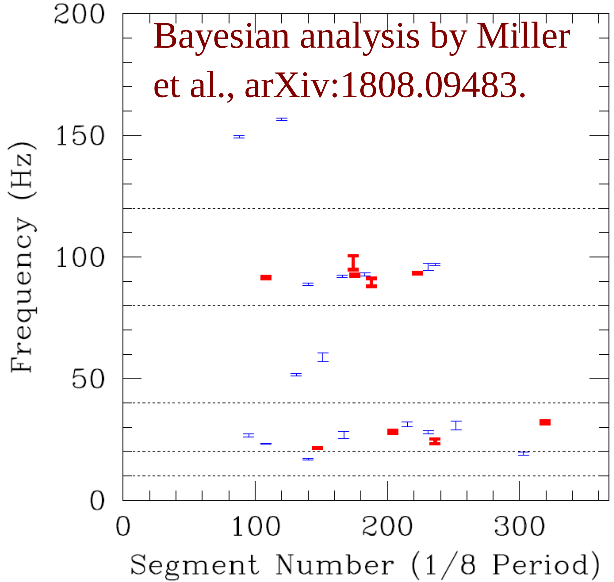

Bayesian analysis by Miller et al., arXiv:1808.09483.

More on magnetar QPOs: Bayesian QPO analysis and “lasagna-sandwich” model

Ref. Sotani et al., arXiv:1906.06999.

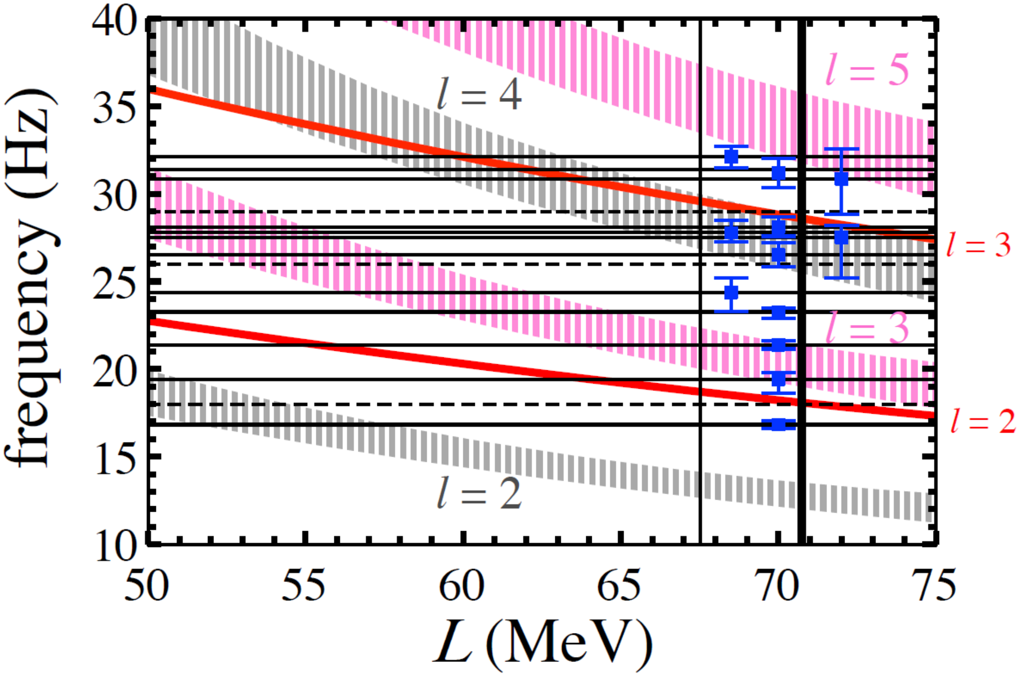

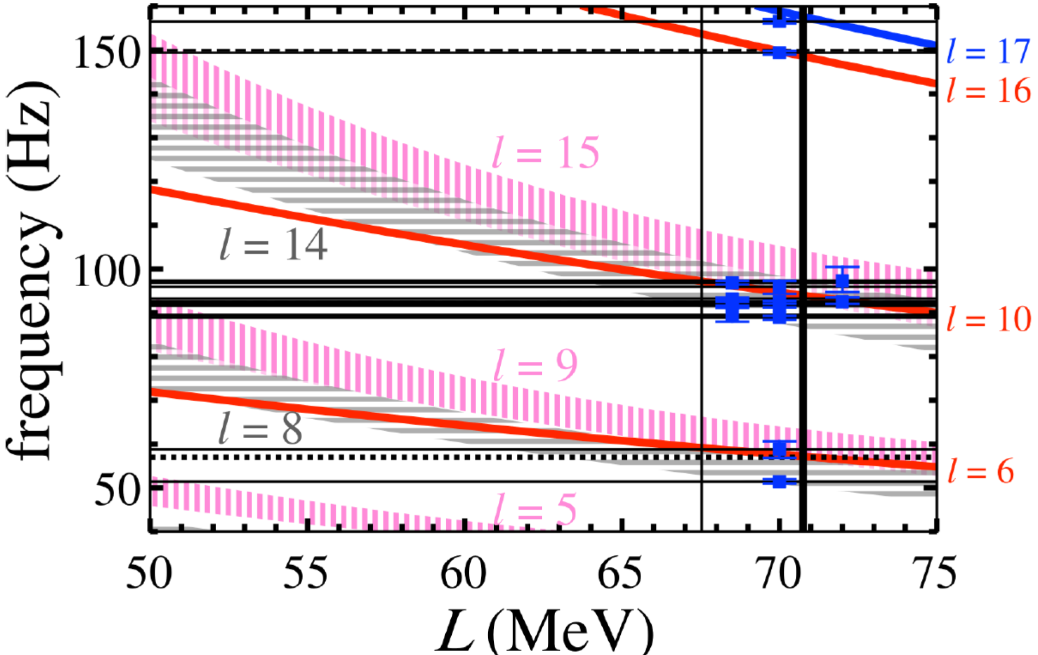

QPO (Hz)	Δf (Hz)	SP+C	CH+SH
18	1.9 ± 0.2	$\ell = 2$	
26	3.0 ± 0.2		$\ell = 4$
29	4.1 ± 0.5	$\ell = 3$	
57	4.4	$\ell = 6$	
92.5	$1.7^{+0.7}_{-0.4}$	$\ell = 10$	
150	17 ± 5	$\ell = 16$	
16.83	0.51	$\ell = 2$ (?)	
19.42	**3.42**		$\ell = 3$
21.38	0.51		$\ell = 3$ (?)
23.26	0.51	?	?
24.38	**4.19**		$\ell = 4$ (?)
26.51	**2.03**		$\ell = 4$
27.52	1.28	$\ell = 3$	
27.78	1.24	$\ell = 3$	
28.11	1.38	$\ell = 3$	
30.85	**5.43**		$\ell = 5$
31.19	**1.90**		$\ell = 5$
32.12	**1.93**		$\ell = 5$
51.40	0.52		$\ell = 8$
58.81	**5.36**	($\ell = 6$)	$\ell = 9$
88.90	0.73		$\ell = 14$
89.51	**4.78**		$\ell = 14$
91.58	1.14	$\ell = 10$	
92.09	0.82	$\ell = 10$	
92.47	0.69	$\ell = 10$	
92.49	0.71	$\ell = 10$	
93.21	0.50	$\ell = 10$	
95.90	**3.74**		$\ell = 15$
96.82	0.60		$\ell = 15$
97.31	**5.94**		$\ell = 15$
149.41	0.79	$\ell = 16$	
156.59	1.14	$\ell = 17$	

Conclusion

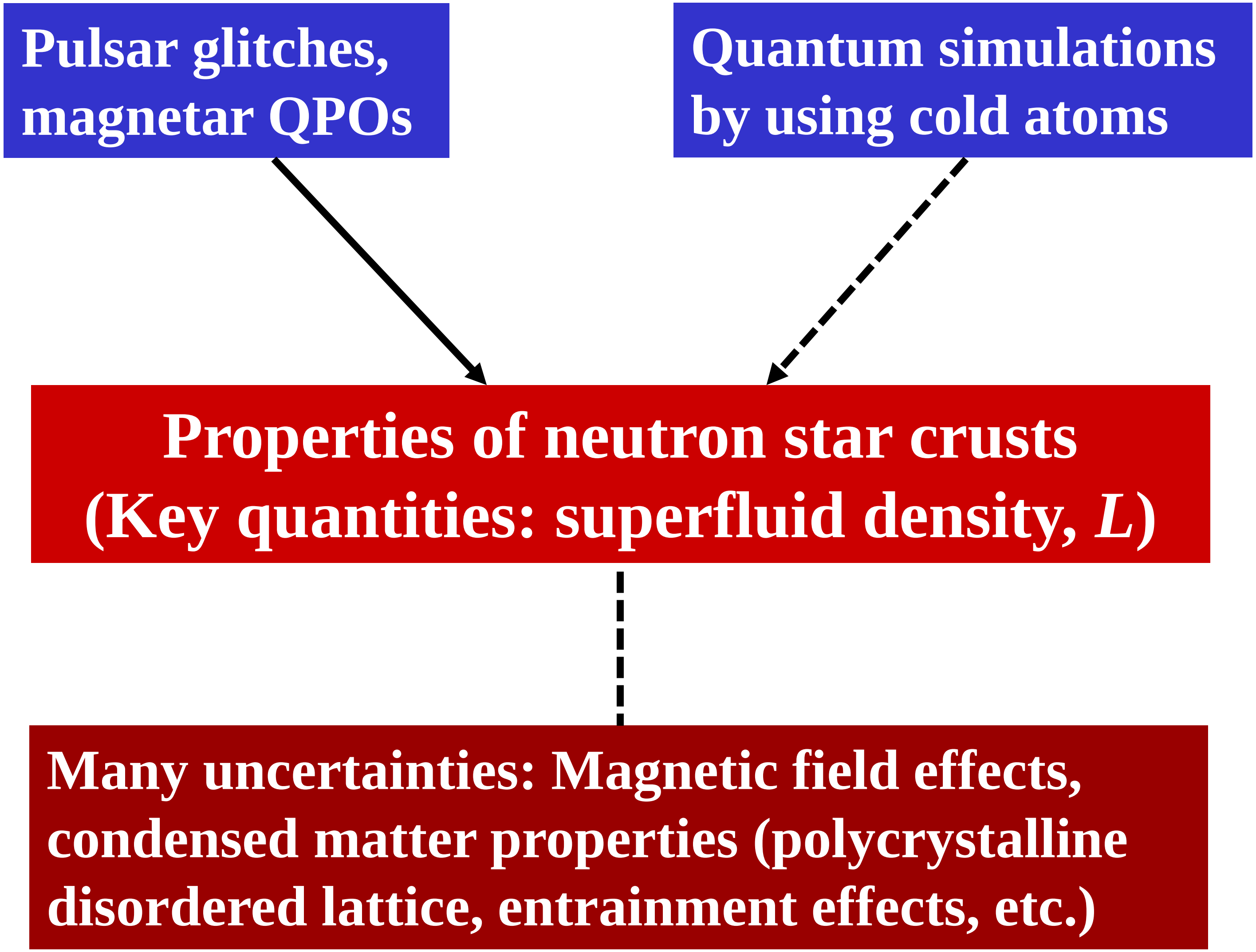

Pulsar glitches,
magnetar QPOs

Quantum simulations
by using cold atoms

Properties of neutron star crusts
(Key quantities: superfluid density, L)

Many uncertainties: Magnetic field effects, condensed matter properties (polycrystalline disordered lattice, entrainment effects, etc.)